1   **Research Article**

2

3   **Bone remodeling in the longest living rodent, the naked mole-rat: interelement variation**

4   **and the effects of reproduction**

5

6   Germán Montoya-Sanhueza[a,b*], Nigel C. Bennett[c], Maria K. Oosthuizen[c], Christine M. Dengler-

7   Crish[d], Anusuya Chinsamy[a]

8

9   [a]*Department of Biological Sciences, University of Cape Town, Private Bag X3, Rhodes Gift 7701, South Africa.*
10   [b]*Department of Zoology, Faculty of Science, University of South Bohemia, Branišovská 1760, České Budějovice*
11   *37005, Czech Republic.*
12   [c]*Mammal Research Institute, Department of Zoology and Entomology, University of Pretoria, Pretoria 0002,*
13   *South Africa.*
14   [d]*Department of Pharmaceutical Sciences, Northeast Ohio Medical University, Rootstown, OH, USA.*
15

16   *Corresponding author: GM-S, getamoo@gmail.com

17

18

19

20

21

22

23

24

25

26

27

28

29

30

31

32

33

ABSTRACT

The pattern of bone remodeling of one of the most peculiar mammals in the world, the naked mole-rat (NMR) was assessed. NMRs are known for their long lifespans among rodents and for having low metabolic rates. We assessed long-term *in vivo* bone labeling of subordinate individuals, as well as the patterns of bone resorption and bone remodeling in a large sample including reproductive and non-reproductive individuals ($n = 70$). Over 268 undecalcified thin cross-sections from the midshaft of humerus, ulna, femur and tibia were analyzed with confocal fluorescence and polarized light microscopy. Fluorochrome analysis revealed low osteogenesis, scarce bone resorption and infrequent formation of secondary osteons (Haversian systems) (i.e. slow bone turnover), thus most likely reflecting the low metabolic rates of this species. Secondary osteons occurred regardless of reproductive status. However, considerable differences in the degree of bone remodeling were found between breeders and non-breeders. Pre-reproductive stages (subordinates) exhibited quite stable skeletal homeostasis and bone structure, although the attainment of sexual maturity and beginning of reproductive cycles in female breeders triggered a series of anabolic and catabolic processes that up-regulate bone turnover, most likely associated with the increased metabolic rates of reproduction. Furthermore, bone remodeling was more frequently found in stylopodial elements compared to zeugopodial elements. Despite the limited bone remodeling observed in NMRs, the variation in the pattern of skeletal homeostasis (interelement variation) reported here represents an important aspect to understand the skeletal dynamics of a small mammal with low metabolic rates. Given the relevance of the remodeling process among mammals, this study also permitted the comparison of such process with the well-documented histomorphology of extinct therapsids (i.e. mammalian precursors), thus evidencing that bone remodeling and its endocortical compartmentalization represent ancestral features among the lineage that gave rise to mammals. It is concluded that other factors associated with development (and not uniquely related to biomechanical loading) can also have an important role in the development of bone remodeling.

1.   INTRODUCTION

Bone remodeling is the mechanism by which old bone is replaced by new bone by the sequential and coupled action of bone resorbing cells (osteoclasts) and bone forming cells (osteoblasts) at single bone sites (Frost, 1969, 1987; Jaworski, 1992; Parfitt, 2010; Seeman, 2008; Allen & Burr, 2014; Currey et al., 2017). Due to the coordinated activity of osteoclasts and osteoblasts, this process results in the formation of secondary osteons (= Haversian Systems) (Enlow, 1962; Jaworski, 1992; Currey et al., 2017) and is usually referred to as secondary reconstruction (Amprino, 1948; Enlow, 1962; Chinsamy-Turan 2005, 2012a). Bone remodeling and secondary osteons (SOs) occur principally along endosteal, intracortical and trabecular bone surfaces (Singh & Gunberg, 1971; Enlow, 1963; Parfitt, 2010; Seeman, 2008; McFarlin et al., 2008; Allen & Burr, 2014). SOs can be found isolated, forming small groups or forming dense groups (Jaworski, 1992; Hillier & Bell, 2007). When dense aggregations of SOs accumulate through several generations and cover a defined bone surface, this is called dense Haversian bone tissue and represents a specific subtype of – secondary-- bone, usually present in large vertebrates (Enlow, 1963; de Ricqlès et al. 1991; Jaworski, 1992; Francillon-Vieillot et al. 1990; Chinsamy-Turan 2005). SOs have been described for a wide range of vertebrates (Foote 1916; Enlow & Brown, 1956, 1958; Enlow, 1969), as well as for all the main mammalian lineages including the most diverse of them, Rodentia (Foote 1916; Ruth, 1953; Enlow, 1962; Jowsey, 1966; Singh & Gunberg, 1971; Singh et al., 1974; Jaworski, 1992; Locke, 2004; Montoya-Sanhueza, 2010; Straehl et al., 2013; Enlow & Brown, 1958; Currey et al., 2017; Felder et al., 2017).

The functions of bone remodeling have been extensively studied and can be grouped into two main roles, which are not mutually exclusive: i) a biomechanical role, as a process of self-repair responsible for the removing of microdamage accumulated in bone material and which is subsequently replaced with new material to avoid fatigue fracture (Frost, 1987a; Currey, 2002; Pearson & Lieberman, 2004; Currey et al., 2017); and ii) as a metabolic regulator of the skeleton to assist with mineralization levels and calcium homeostasis (Amprino, 1948; Currey, 2002; Parfitt, 2010; Doherty et al., 2015). An additional function of SOs has also been associated with the development of bone tuberosities and sites of muscle attachment during the process of bone growth and relocation (Enlow, 1963; McFarlin et al, 2008; Parfitt, 2010). Thus, bone remodeling is a fundamental process for the postnatal development of the skeleton aiding in keeping material properties and balanced mineral homeostasis of the adult skeleton. Eventually, altering bone remodeling's normal function and activity may lead to

99   several osteopathies including osteoporosis, whereby understanding the causes (etiology) and

100 mechanisms of bone remodeling represents a major goal in bone biology research (e.g.

101 Agarwal & Stout, 2003; Parfitt, 2010; Bonucci & Ballanti, 2014; Doherty et al., 2015; Currey

102 et al., 2017; Piemontese et al., 2017).

103 Most of our knowledge on bone remodeling comes from investigations on laboratory rodents

104 and humans, both of which exhibit a distinct pattern of remodeling. Humans develop highly

105 remodeled bones forming dense Haversian tissue in adulthood (Goldman et al., 2009

106 Cambra-Moo et al., 2014), whereas mice (*Mus musculus*) and rats (*Rattus norvegicus*)

107 develop scarce and isolated SOs during their relatively shorter lives (Enlow & Brown, 1958;

108 Singh & Gunberg, 1971; Forwood & Parker, 1986). Such disparate patterns have obscured

109 our attempts to understand the functions of bone remodeling among mammals, probably

110 because other factors such as body size and phylogenetic signal (which are still poorly

111 understood) are also relevant in explaining this process. Recently, a series of studies

112 described the complete lack of SOs and bone remodeling in the naked mole-rat (NMR),

113 *Heterocephalus glaber* (Currey et al., 2017; Carmeli-Ligati et al., 2019), a small mammal that

114 can live for up to 30 years in captivity and exhibits the longest lifespan of any rodent known

115 to science (Sherman & Jarvis, 2002; Dammann & Burda, 2007). However, Montoya-

116 Sanhueza et al. (*in press*) reported and illustrated conclusive evidence for the development of

117 SOs in *H. glaber*.

118 Montoya-Sanhueza et al. (*in press*) also reported that bone remodeling comprised a limited

119 process among subordinates and that SOs appeared mainly in the humerus and femur and to a

120 lesser extent in the ulna and tibia, thus suggesting a differential pattern of bone remodeling

121 between stylopodial and zeugopodial bones. Information documenting similar patterns in

122 extant vertebrates is scarce and dispersed, e.g. testudines (Bhat et al., 2019), equids

123 (Nacarino-Meneses et al., 2016), caprinids (Cambra-Moo et al., 2015), primates (Warshaw,

124 2008). Surprisingly, additional reports come from archeological and paleontological studies

125 describing differences between bones in past human populations (Mulhern, 2000; Cho &

126 Stout, 2011), as well as in a diverse range of extinct vertebrates such as non- mammalian

127 therapsids, equids, elephant birds and dinosaurs (e.g., Cullen et al., 2014; Martinez-Maza et

128 al., 2014; Padian et al., 2016; Chinsamy et al., 2020). Despite the incidence of this

129 phenomenon in a diverse group of vertebrates, there is a considerable gap in our

130 understanding of the causes leading to differential skeletal homeostasis among these taxa.

131   In order to increase our knowledge on this process among small mammals, we assessed the

132   extension and amount of bone remodeling (i.e. formation of secondary osteons) in the long

133   bones of NMRs. We assessed prolonged *in vivo* bone labeling in non-reproductive

134   individuals, as well as analyzed a large sample of reproductive and non-reproductive

135   individuals to assess the effects of reproduction on their bone microstructure. It is known that

136   mammalian reproduction encompasses strong metabolic effects on the endochondral and

137   intramembranous osteogenesis of females (Redd et al., 1984; Miller et al., 1986; Vajda et al.

138   2001; Miller & Bowman, 2004). In NMRs, it has been reported that male and female

139   subordinates are sexually monomorphic with no significant differences in skeletal phenotype

140   (Pinto et al. 2010), although the cortical and trabecular bone structure, as well as its bone

141   quality are significantly lower in subordinate females than in female breeders (Dengler-Crish

142   & Catania, 2007; Pinto et al. 2010). Similarly, anabolic changes (bone formation) in

143   trabecular bone (lumbar spine) of NMRs have been reported across pregnancy and lactation

144   (Dengler-Crish & Catania 2007, 2009; Henry et al., 2007), while Pinto et al. (2010) also

145   mentioned extensive catabolic activity (i.e. bone resorption) in females during late pregnancy

146   and lactation. These studies demonstrate the female breeders of NMRs experience

147   considerable changes in their skeletal homeostasis, although none of these studies have

148   assessed the pattern of mineral mobilization, bone resorption and bone remodeling at the

149   microstructural level. Therefore, additional studies on the bone dynamics and bone histology

150   of NMRs during reproduction are also needed. This study allowed us to assess the process of

151   bone remodeling in NMRs, thus expanding our knowledge on the function and causes of this

152   process in small mammals.

153

154   **Naked mole-rats: a novel model to study bone dynamics**

155   NMRs are small (~34 g) subterranean mammals characterized by having slow somatic

156   growth, low metabolic rates and low basal body temperatures as compared to other mammals

157   (Buffenstein & Yahav, 1991; O'Riain, 1996; Bennett et al., 1991; Jarvis & Sherman, 2002;

158   Zelová et al., 2007; Šumbera, 2019; Braude et al., 2020; Buffenstein et al., 2020). They live

159   in large eusocial colonies (averaging 78 individuals) typically composed of one breeding

160   female (queen) and 1-4 reproductive males, while the rest of the colony members

161   (subordinates) remain reproductively suppressed and therefore having a hypogonadic

162   condition (Sherman et al., 1992; Jarvis & Sherman, 2002; Braude et al., 2020). They excavate

163 extensive burrow systems in arid habitats with hard and solidified soils (Jarvis & Sherman,

164 2002; Holtze et al., 2008), principally aided with their chisel-like incisors and secondarily by

165 their fore- and hindlimbs, so that their long bones are expected to experience high strains

166 during tunnel excavation. However, several studies have revealed that despite these factors

167 (i.e. energetically demanding foraging/locomotor strategy and hypogonadic condition of

168 subordinates), their femora maintains high bone structure and mechanical properties for most

169 of their lifespan (e.g. Pinto et al., 2010; Edrey et al., 2011; Carmeli-Ligati et al., 2019;

170 Montoya-Sanhueza et al. *in press*). This was also confirmed for the humerus, ulna and tibia,

171 thus evidencing a systemic functional adaptation to principally withstand the mechanical

172 strains imposed during digging behavior (Montoya-Sanhueza et al. *in press*).

173 Additionally, the breeding female can have multiple litters in one year, comprising of up to

174 27 pups per litter (average of 12 young per litter) (Bennett et al., 1991; Jarvis, 1991; Hood et

175 al., 2014). This suggests that the patterns of mineral mobilization during reproduction may

176 considerably affect the skeletal homeostasis of female breeders in order to ensure sufficient

177 mineral resources destined for skeletal development of young. Hood et al. (2014) found that

178 the milk of the breeding female is rather diluted (i.e. having a high water content) in

179 comparison to other rodents, although they have higher calcium to phosphorus (Ca : P) ratios

180 relative to other rodent milks, probably associated with high levels of mineral mobilization

181 from bones. For these reasons, NMRs represent a unique model to assess the mechanisms

182 involved in the delayed senescence of their skeletal system, particularly their age-related

183 bone loss and reproductive-related skeletal homeostasis (e.g. O'Connor et al., 2002; Pinto et

184 al., 2010; Buffenstein et al., 2012).

185

2.   MATERIAL AND METHODS

187 Reproductive (n = 6) and non-reproductive (n = 64) adults of both sexes were studied (Table

188 1). Specimens were derived from captive colonies kept at the University of Cape Town

189 (UCT), University of Pretoria (UP) and Northeast Ohio Medical University (NOMU). For

190 complete ontogenetic information and housing details of individuals see Montoya-Sanhueza

191 et al. (*in press*). Ethical approval for the specimens #156-164 from the NEOMED

192 Institutional Animal Care and Use Committee in accordance with the Guide for Care and Use

193 of Laboratory Animals published by the National Institutes of Health. For further

194   identification of the individuals of this study we used the last three numbers of their ID codes

195   (Table 1).

196   In order to illustrate the morphological variation within our sample, body mass (BM) and

197   femoral length (FL) were measured. BM of specimens #155-164 and #506-511 were obtained

198   immediately following death, whilst the BM of the rest of the specimens was obtained after

199   defrosting them, so this data could be underestimated and therefore should be interpreted with

200   caution (Table 1; Fig. 1A). A standard electronic balance (0.01 g) was used to measure BM.

201   Some specimens presented missing arms, legs or open stomachs when collected from

202   colonies, so these specimens were not included in Figure 1A. FL was measured using a

203   Mitutoyo digital caliper (0.01 mm) and corresponds to the total length of the femur from its

204   proximal articular surface to the distal one. This measure was obtained for almost all

205   individuals and has been incorporated in previous studies of NMRs (e.g. Pinto et al., 2010;

206   Carmeli-Ligati et al., 2019), thus representing a good element for further comparisons. To

207   visualize the distribution of body sizes within the sample, BM was plotted against FL using

208   ordinary least square (OLS) regression (Fig. 1A).

209

210   <Table 1>

211

212   Since the epiphyses of mice and rats typically remain unfused during their relatively short

213   lives and even after somatic maturity is attained (Parfitt, 2002a; Roach et al., 2003; Farnum,

214   2007; Geiger et al., 2014), these are considered poor estimators of skeletal maturity among

215   rodents. However, because the extreme longevity of NMRs, it would be interesting to assess

216   if this species follows a similar pattern. More importantly, the estimation of epiphyseal fusion

217   may contribute to the determination of endochondral (longitudinal) growth sequences and

218   therefore potential patterns of interelement variation in this species. Both proximal and distal

219   epiphyses were measured and classified into one of the three categories depending on the

220   degree of epiphyseal fusion; non-fused (NF), half-fused (H) and fused (F) (Table S1). Thus,

221   this parameter provided an estimate of growth plate closure and definitive cessation of

222   endochondral ossification. When both epiphyses showed either a fused or half-fused

223   condition this was referred to as double fusion and the bone was considered to have ceased its

224   longitudinal growth and then classified as a non-growing bone (nGB) (Table S1).

225

226   <Table S1>
227

228   2.1   *In Vivo* Bone Labeling

229   Nine randomly selected mature individuals from colonies kept at UP were injected with three

230   different fluorochromes over a period of ~10 months (Table 2; Fig. 1B). This sequence

231   permitted tracking osteogenesis along almost an annual cycle, which to our knowledge it

232   represents the first study assessing long-term bone dynamics in a small mammal. A previous

233   study on a small primate, the grey mouse lemur, *Microcebus murinus* (60–80 g), assessed

234   osteogenesis for a period of 20 days (Castanet et al., 2004). Rabey et al. (2015) assessed the

235   effects of activity on bone osteogenesis in laboratory mice (~34 g) which were injected three

236   times over a period of 28 days in an experiment that lasted 78 days. Individuals in our study

237   were identified by using subcutaneous Passive Integrated Transponder (PIT) tags (except the

238   queen #506). Out of nine specimens tagged, four of them lost their PIT tags so those

239   specimens were not retrieved.

240   The three fluorochromes were administrated intramuscularly in the leg after the 6th and 4th

241   months from the first injection (Table 2; Fig. 1B): Engemycin-Oxytetracycline (10%) (Ot),

242   Alizarin (complexone) red (Ar) and Calcein (Cn), which respectively fluoresces yellow, red,

243   and green (Table 2). Further details of the fluorochrome labeling procedure are presented in

244   Table 2. Unfortunately, the queen died before injecting the last two fluorochromes. It is

245   important to note that from the specimens successfully injected, none of them registered the

246   first Ot label. It is likely that the low concentrations of this fluorochrome (Table 2) were not

247   appropriately assimilated by the individuals. For this reason, the histological descriptions are

248   focused only on the last two fluorochromes (Ar and Cn), thus covering a period of seven

249   months from the second injection (Ar) until the specimens were euthanized (Table 2).

250   Fluorochrome labels were detected using confocal fluorescence microscopy (Zeiss LSM 880

251   Confocal - Fast AiryScan Technology) at the Confocal and Light Microscope Imaging

252   Facility of the Faculty of Health Sciences at UCT. All experiments were approved by the

253   Animal Ethics Committee of the University of Pretoria (AEC–UP: EC024-17).

254

255   2.2   Osteohistological Procedures and Nomenclature

256   Undecalcified cross-sections from the midshaft of the diaphysis, i.e. ~50% of the total bone

257   length from the proximal articular surface were prepared at the Department of Biological

258   Sciences at UCT. A total of 268 thin cross-sections of 80–100 μm thickness were analyzed

259   and high-quality photomicrographs were taken with a Nikon Eclipse E200 Polarizing

260   Microscope. The bone histomorphology described here was visualized using conventional

261   transmitted light and polarized light microscopy with a gypsum (¼ lambda) filter and follows

262   the nomenclature of Enlow (1963), Francillon-Vieillot et al. (1990), de Ricqlès et al. (1991),

263   Bromage et al. (2003) and Chinsamy-Turan (2005, 2012a). Additional nomenclatural

264   terminology regarding bone remodeling is provided in Section 2.3. Full description of the

265   osteohistological procedures are also presented in Montoya-Sanhueza et al., (*in press*).

266

267   2.3   Quantification of Bone Remodeling

268   The formation of secondary osteons (SO) in mammals is usually used to estimate their levels

269   of bone remodeling and bone turnover (e.g. Ruth, 1953; Forwood & Parker, 1986; Frost,

270   1987b; Vajda et al., 1999). In larger mammals, these quantifications are based on the

271   extension of bone surface covered by secondary bone (e.g. osteon population density, Frost,

272   1987b; Cho & Stout, 2011; Martinez-Maza et al., 2014). Because SOs in subordinate NMRs

273   are not highly abundant and they never form dense Haversian bone (Montoya-Sanhueza et

274   al., *in press*), we quantified the total number of SOs per cross-section in each bone element.

275   This information allowed us to know which bones are most frequently remodeled, as well as

276   compare the total density of SOs between bones.

277   The first phases of bone remodeling can be structurally identified by the formation of

278   resorption cavities (RC), which occurs when osteoclasts remove both matrix and minerals

279   from bone (Sissons et al., 1984). This cellular activity results in the formation of Howship's

280   lacunae which are eroded surfaces with scalloped borders in the cortex (Sissons et al., 1984).

281   Bone resorption is followed by osteoid formation, which is ultimately mineralized and

282   consequently results in the formation of a SO. SOs can be recognized by a series of

283   histological features including: i) delimited margins or cement/reversal line; ii) a Haversian

284   canal; and iii) concentric lamellae with osteocytes deposited around the Haversian canal (de

285   Ricqlès et al. 1991; Jaworski, 1992; Martin et al., 1998; Currey, 2002). However, SOs exhibit

286   high variation in their size, shape and frequency among mammals. For example, Felder et al.

287   (2017) recently reported that larger mammals have larger osteonal and Haversian canal areas

288   as compared to smaller mammals (in absolute terms), although these parameters are smaller

289   in larger mammals (in relative terms) and scale with negative allometry. This variation may

290   be associated with the bone surface (endosteal or periosteal envelopes) and region

291   (endocortical, intracortical or pericortical) in which it develops (e.g. Thomas et al., 2005;

292   Kim et al., 2015), as well as have an ontogenetic (Maggiano et al., 2016) and genetic basis

293   (Havill et al., 2013). SOs can also exhibit incomplete remodeling associated with its

294   development, i.e. "secondary osteon's ontogeny" (Jaworski, 1992; Kearns et al., 2008;

295   Andersen et al., 2013; Maggiano et al., 2016). Thus, one SO can contain both a resorptive

296   surface and a mineralizing surface at the same time, and therefore its Haversian canal may

297   appear not fully developed. This has been called as the reversal osteon, resorbing osteon or

298   simply immature osteon (e.g. Mori & Burr, 1993; Vajda et al., 1999; Montoya-Sanhueza &

299   Chinsamy, 2017). Given the morphological variation found within a complete SO in

300   mammals, this study does not make a distinction between specific morphologies and consider

301   a SO as having a cement line surrounding recently formed bone and a Haversian canal or an

302   eroded canal, both which indicate centripetal bone formed around a vascular canal. For these

303   reasons, to estimate the degree of bone remodeling in this study we described and quantified

304   the development of mature and immature SOs, regardless shape and location (e.g. Montoya-

305   Sanhueza & Chinsamy, 2018). Significantly large RCs undergoing secondary reconstruction

306   were not considered as secondary osteons *per se*, but were also included in the qualitative

307   descriptions since they represent extensive catabolic activity followed by more recent

308   anabolic activity (Montoya-Sanhueza & Chinsamy, 2018, and references therein).

309

3.   RESULTS

311

312   The mean body mass (BM) of the injected subordinates at the end of the experimental period,

313   excluding the breeding female (#506), was 35.60 g ($n = 5$), a value which is between the

314   lightest (17.72 g) and heaviest (66 g) subordinates of the sample (Table 1; Fig. 1A). BM

315   increased during the ~10 months of the labeling experiment, except in the individual #508,

316   which maintained an unchanged BM (Table 2; Fig. 1B). The mean femoral length (FL) of the

317   injected specimens was 14.01 mm ($n = 5$), which is between the shorter (11.60 mm) and

318   longest (16.47 mm) femora within the sample (Table 1; Fig. 1A). The mean BM and FL of

319   the rest of the subordinates (excluding known-age specimens #156-164) was 32.23 g ($n = 27$)

320   and 14.30 mm ($n = 30$) for females and 33.26 g ($n = 18$) and 14.66 mm ($n = 22$) for males,

321   respectively. In general, these data showed that adult subordinates varied considerably in BM

322   and that the injected individuals (of intermediate size) were still growing (Fig. 1B). The OLS

323   between BM and FL presented a low coefficient of determination ($R^2 = 0.23$, Fig. 1A).

324   Considerable variation in BM was still present (low $R^2 = 0.49$) when only the subordinates

325   from UCT colonies were plotted. In breeders, the mean BM and FL were 36.60 g ($n = 4$) and

326   14.87 mm ($n = 6$), respectively (Fig. 1A). The min /max values for BM and FL of breeders

327   were 16.04/56.60 and 13.95/15.72, respectively, thus also showing a high variation in BM

328   (Table 1).

329

330   <Table 2>

331

332   <Figure 1>

333

334   3.1 *In vivo* bone labeling

335   The five subordinates (#507-511) injected with fluorochromes did not exhibit considerable

336   differences in their bone matrix composition and/or main arrangement of bone tissues, and

337   they did not differ considerably from the bone histology of the larger sample of subordinates.

338   3.1.1   Humerus

339   This bone showed thick cortical walls and varied degrees of intracortical resorption in the

340   anterolateral side (Fig. 2A). Fluorochrome labels indicating bone activity were few and

341   appeared in the endocortical region, trabeculae and to a lesser extent in the intracortical

342   region (associated with osteonal formation), with no labels observed in the pericortical region

343   (Table 2; Fig. 2A). Thus, periosteal bone formation (growing in diameter) had apparently

344   ceased during the experimental period (last seven months) in this bone. The specimens #510

345   showed clear evidence of osteonal activity: the fluorochrome label was deposited

346   centripetally in one side of a resorption cavity (RC) and its mineralized osteoid contained

347   small osteocyte lacunae compared to the larger osteocyte lacunae of the surrounding lamellar

348   bone (LB) matrix (Fig. 2B). Most labels in the humerus were deposited within LB of

349   endocortical regions and associated with resorption lines (RL), thus indicating secondary

350   reconstruction of endosteally deposited tissues (Fig. 2C).

351   One of the smaller specimens (#511) showed more endosteal activity as compared to the

352   other specimens (Fig. 2A, C). The bone histology of this specimen showed the clearest signs

353   of cortical drift among all the labeled specimens, consisting of: i) bone apposition in the

354   endocortical region (medial side); and ii) endosteal bone resorption in the opposite (lateral)

355   side, thus indicating cortical drift towards the lateral side of the diaphysis.

356   In general, these data suggests that bone modeling in the humerus has mostly ceased and that

357   most of the bone formation has been attained prior to the experimental period, although bone

358   remodeling is still active at intracortical and endocortical surfaces. Additionally, the

359   permanence of double labels in the trabeculae over a period of seven months (Fig. 1B)

360   indicates low rates of bone resorption.

361   The quantification of SOs in subordinates showed that 50% of the humeri analyzed exhibited

362   at least one SO (Table 3). The maximum number of SOs per individual was six, mostly

363   associated with the anterolateral side of the humerus.

364

365   <Figure 2>

366

367   <Table 3>

368

369   3.1.2   Ulna

370   In general, the ulna showed reduced intracortical and endosteal bone resorption, which often

371   resulted in an almost completely occluded MC and a highly compacted cortex (Fig. 3A).

372   Only two individuals showed fluorochrome labels (Table 2), which were very limited in

373   extension and mostly associated with endocortical LB (posterior side) (Fig. 3A). Only one

374   specimen (#507) showed a periosteal label on the lateral side, indicating cortical drift towards

375   this region. This indicates that periosteal bone growth has mostly ceased in the ulna of the

376   injected individuals and that most of the bone formation was attained prior to the

377   experimental period. The low resorptive and osteogenic activity of this bone contrasts with

378   the relatively higher bone turnover of the humerus.

379   SOs in the ulna of subordinates was considerably lower than in the humerus and only 5.36%

380   of the individuals exhibited at least one SO (Table 3). The maximum number of SOs per

381   individual was three, mostly associated with the anterior side of the bone.

382

383   <Figure 3>

384

385   3.1.3   Femur

386   This bone showed thick cortical walls and some trabeculae in the endocortical region (Fig.

387   4A). Fluorochrome labels appeared associated to the trabeculae and endocortical regions

388   (medial and lateral sides), as well as in the pericortical region, at the tip of the lateral side

389   (Table 2; Fig. 4A, B). The few bone labels found in the pericortical region indicated that

390   radial bone growth (i.e. bone modeling) was still occurring when fluorochromes were

391   injected. The limited activity observed in the trabeculae and endocortical regions evidenced

392   low remodeling activity (and slow bone turnover) of these surfaces, since the labels were

393   maintained for the last seven months (Table 2). Labels were associated with lines of arrested

394   growth (LAGs) and LB (Fig. 4B, D, E), indicating cyclical and slow bone deposition,

395   respectively. The femur also showed clear evidence of osteonal remodeling: fluorochrome

396   labels were deposited centripetally on one side of an eroded vascular canal (VC), containing

397   mineralized osteoid with small osteocyte lacunae compared to the osteocyte lacunae of the

398   surrounding LB matrix (Fig. 4C). The femur of the specimen #511 showed more endosteal

399   bone formation as compared to the rest of the specimens (Fig. 4D), similar to the

400   observations made for the humerus of the same individual (Fig. 2C). In general, the bone

401   histology of this and other specimens showed bone apposition in the lateral side, in

402   endocortical regions of the anterior, medial and sometimes lateral sides, as well as endosteal

403   resorption in the posterior side (Fig. 4B, D-E). This indicated cortical drift towards the lateral

404   and posterior side of the diaphysis.

405   The number of SOs quantified in the femur of subordinates was considerably lower as

406   compared to the humerus. Only the 14.52% of the femora analyzed exhibited at least one SO

407   (Table 3). The maximum number of SOs per individual was two, mostly associated with the

408   lateral side of the bone.

409

410   <Figure 4>

411

412   3.1.4   Tibia

413   This bone exhibited a highly compacted bone with a small MC (Fig. 3B). Fewer

414   fluorochrome labels were observed in this bone as compared to the femur (Table 2). This

415   indicates that most of the bone growth of the tibia occurred before the experimental period.

416   This bone recorded mostly the last Cn label in endocortical regions, although the specimen

417   #511 also exhibited a thin Ar label in a localized area of the pericortical region (Fig. 3B). The

418   minimal periosteal activity of this bone indicates that radial bone growth has apparently

419   ceased during the experimental period. Likewise, the minimal presence of RCs in the injected

420   specimens indicates that this bone experience a slower bone turnover as compared to the

421   femur.

422   The tibia of subordinates showed the lowest quantity of SOs and only the 4.92% of the tibiae

423   exhibited at least one SO (Table 3). The maximum number of SOs per individual was one.

424

3.2   Bone Remodeling in Breeders

426   All breeders (6) exhibited similar bone matrix composition and bone tissue distribution as

427   compared to non-breeding subordinates. However, breeders exhibited a wider variation in

428   bone microanatomy, cortical porosity and secondary reconstruction (bone remodeling) of

429   endocortical and intracortical surfaces as compared to subordinates. This resulted in some

430   individuals with considerable thinning of cortical walls, as well as in extreme

431   trabecularization and enlargement of MCs (Fig. 5A). Three breeders showed high levels of

432   bone resorption and secondary reconstruction (i.e. #072, #089, #506), not comparable to the

433   observed histomorphological pattern of subordinates. The other breeders (#051, #498, #155)

434   showed scarce to moderate bone resorption. Among all the bones analyzed, the humerus was

435   the most affected by remodeling, specifically the anterolateral region (e.g. #506, Fig. 5B).

436   This region is normally remodeled in subordinates (e.g. #507, #511; Fig. 2A), although this

437   process is accentuated in some breeders, reaching high trabecularization (Fig. 5A). This was

438   evidenced by extensive endosteal and intracortical resorption forming enlarged RCs, often

439   followed by secondary reconstruction (Fig. 5B). The ulna of breeders also showed endosteal

440   resorption, but this bone is less altered as compared to the humerus. The femur exhibited

441   considerable thinning of their cortical walls (Fig. 5A, D). Although the femur usually lacks

442   trabecular development in subordinates (e.g. #507; Fig. 4A), some breeders showed active

443   endosteal resorption (e.g. #498) to considerable trabecularization of the MC (e.g. #072; Fig.

444   5A). In the tibia, increased intracortical resorption, endocortical trabecularization and

445   expansion of the MC was also observed, but this bone also appeared less altered than the

446   femur. In general, apart from the endocortical and intracortical regions, the pericortical region

447   did not exhibit considerably alterations in breeders.

448   The development of SOs in breeders followed a similar pattern as in subordinates, although

449   these were present only in two individuals (Table 3). Thus, 20% of the humeri and femora

450   analyzed exhibited at least one SO (Table 3). The ulna and tibia of breeders did not present

451   SOs. The bones of the specimen #072 showed highly resorbed bone sections, so no SOs were

452   discernible.

453

454   <Figure 5>

455

456   3.3 Epiphyseal Fusion

457   Most individuals presented unfused epiphyses and only a few of them of different body sizes

458   showed simultaneous double fusion (of both proximal and distal epiphyses), thus indicating

459   that such bones have completely ceased their longitudinal growth (Fig. 1A; Table S1). Figure

460   1A illustrates the dispersed distribution of the individuals presenting non-growing bones

461   (nGB). In general, the forelimb presented more cases of double fusion (14) than the hindlimb

462   (8). In the forelimb, double fusion was highly frequent in the ulna (12 cases) and least

463   frequent in the humerus (2 cases), whereas in the hindlimb, this was slightly more frequent in

464   the femur (5 cases) than the tibia (3 cases). Some individuals of known-age showed double

465   fusion, the breeder of 2.83 years (humerus, ulna and femur, #155) and two subordinates of

466   2.67 (ulna, #157) and 2.50 (femur and tibia, #158) years, thus indicating that cessation of

467   longitudinal growth for these bones has already occurred before the third year of life,

468   regardless attainment of sexual maturity. None of the injected individuals presented double

469   fusion. However, half of the breeders exhibited at least one double fusion of their long bones,

470   predominantly the ulna.

471

4.   DISCUSSION

473   In this study we described the process of bone remodeling of a large sample of subordinate

474   and reproductive individuals of *Heterocephalus glaber*. Prior to this study, varied information

475   existed about the pattern of bone remodeling of this species, principally regarding the

476   assumptions that this species exhibited either a high level of bone remodeling or a complete

477   lack thereof. Similarly, the bone microstructure and pattern of bone remodeling of

478   reproductive individuals remained unknown. The multidisciplinary analysis of a large

479   number of individuals including *in vivo* bone labeling of subordinates, histomorphological

480   assessment of bone remodeling and analysis of epiphyseal fusion allowed us to present

481   conclusive evidence for i) the development of secondary osteons (SOs) in *H. glaber*

482   (regardless of sex and sexual maturity) (Fig. 2B), ii) the level of bone remodeling in different

483   bone elements, as well as iii) the presence of extensive reproduction-related secondary

484   remodeling in female breeders (Fig. 5B). Interspecific comparisons with extant rodent

485   models, as well as with extinct taxa allowed us to hypothesize about the role and ancestrality

486   of this process within the therapsid-mammalian lineage.

487   The development of secondary osteons in all bones analyzed demonstrated that bone

488   remodeling is indeed quite limited in NMRs (Table 3), but not non-existent as previously

489   suggested (Currey et al., 2017; Carmeli-Ligati et al., 2019). Based on the findings of this and

490   a previous study (Montoya-Sanhueza et al., *in press*) we discard the claims that NMRs

491   possess either many SOs or completely lacks them. The fact that a large number of

492   individuals did not present SOs in their midshaft does not preclude them from developing

493   them in other regions of their skeletons, especially in sites or bones typically associated with

494   higher rates of bone turnover as compared to cortical regions, such as the metaphysis of long

495   bones and vertebrae (Parfitt, 2002b).

496   In African mole-rats the development of SOs is not rare and it was initially demonstrated for

497   long bones of the largest bathyergid, the solitary Cape dune mole-rat, *Bathyergus suillus*

498   (Montoya-Sanhueza & Chinsamy, 2017, 2018) and recently confirmed for all the genera

499   within Bathyergidae (Phiomorpha) (Montoya-Sanhueza, 2020). The pattern of SO formation

500   and cortical distribution in NMRs is similar to that described for *B. suillus*, which showed

501   high variation in size and shape and were generally scarce and randomly distributed in

502   intracortical and endocortical regions, usually associated with woven bone and compacted

503   coarse cancellous bone (Montoya-Sanhueza & Chinsamy, 2017). SOs are also present in the

504   Cape porcupine, *Hystrix africaeaustralis* (Hystricidae) (Montoya-Sanhueza, 2020), the

505   largest rodent in Africa, which is a sister group of the clade including NMRs, conformed by

506   Caviomorpha + Phiomorpha (Patterson & Upham, 2014; Upham & Patterson, 2015).

507   However, as also reported for *B. suillus* and other rodents in general (Enlow & Brown, 1958;

508   Jaworski, 1992; Montoya-Sanhueza & Chinsamy, 2017), NMRs do not develop dense

509   Haversian tissue.

510   In general, rodents develop few SOs in their bones (Enlow & Brown, 1958; Enlow, 1963;

511   Forwood & Parker, 1986; García-Martínez et al., 2011). However, they still exhibit typical

512   responses to changing biomechanical and metabolic conditions, thus initiating localized bone

513   remodeling either during increased locomotor activity (e.g. Forwood & Parker, 1986;

514   Bentolila et al. 1998), diet-related mineral deficiency (e.g. Ruth, 1953) or lactation (Ruth,

515   1953; Miller et al., 1986). These data and the observations presented in our study provide

516   additional support to the hypothesis that bone remodeling in small-sized mammalian lineages

517   such as Rodentia may have an important role in calcium regulation and mineral homeostasis.

518   Currey et al., (2017) suggested that the reduced number of SOs in rodents and other small

519   mammals and birds may be due to their short lifespans, which would impede from develop

520   them. However, the existence of few SOs in the long lived NMR refutes this hypothesis, thus

521   indicating that reduced bone remodeling in small mammals occurs regardless lifespan

522   constrains (Currey et al., 2017). The possibility that other constraints such as phylogeny and

523   body size may have more important roles on this phenomenon needs further assessment (e.g.

524   Jaworski, 1992; Currey et al., 2017).

525   Nonetheless, an important factor explaining this phenomenon can be associated with the

526   simple fact that the regions usually undergoing bone remodeling in small mammals (i.e.

527   endocortical regions) are rapidly obliterated during ontogeny thus impeding the record of this

528   process in the adults, which also have thin cortical walls. Based on our findings, African

529   mole-rats maintain thick cortical walls over their lives (Montoya-Sanhueza & Chinsamy,

530   2017; Montoya-Sanhueza, 2020), thus allowing the observation of both ontogenetic and

531   metabolic processes in their bone microstructure. Similarly, several extinct taxa including

532   mammalian precursors and other non-mammalian cynodonts exhibit thick cortical walls with

533   predominance of bone remodeling occurring in their inner endocortical regions (e.g. Botha &

534   Chinsamy, 2004; Ray & Chinsamy, 2004; Ray et al., 2004; Botha-Brink & Angielczyk, 2010;

535   Shelton & Sander, 2017). This indicates the ancestrality of the remodeling process and its

536   regionalization within the therapsid lineage.

537

538   4.1   Scarce Bone Remodeling and Low Osteopenia in *Heterocephalus glaber*

539   Remodeling in subordinates was minimal and mostly associated with the development of a

540   few SOs (1-6) per bone (Table 3). These were usually rounded and relatively small, mainly

541   associated with woven bone or lamellar bone matrices (Fig. 2B). Moreover, the presence of

542   incompletely formed SOs (e.g. Fig. 4C) indicated different stages of osteon maturity. The

543   assessment of *in vivo* bone labeling in subordinates also showed a pattern of reduced bone

544   remodeling and slow bone turnover among mature individuals. Injected specimens exhibited

545   limited bone formation and fluorochrome labels are maintained over an extended period (~7

546   months), thus suggesting a limited resorption of early deposited bone matrices (Fig. 2-4). It is

547   most likely that most of the cortical bone formation in these individuals occurred before the

548   experimental period, when individuals weighed less than 29.8 g on average (Table 2) and that

549   bone modeling in these bones has almost ceased completely, especially in zeugopodial

550   elements. It is possible that previous osteogenic activity at the beginning of the experimental

551   period may not have been recorded due to the inability of recording the first oxytetracycline

552   injection. However, it is unlikely that the osteogenic activity occurring during this period was

553   responsible for the formation of the entire cortex.

554   The scarce bone loss in the long bones of adult NMRs indicates that osteopenia (i.e. intrinsic

555   age-related bone loss) is quite limited, as also noted for other bathyergids (Montoya-

556   Sanhueza & Chinsamy, 2017; Montoya-Sanhueza, 2020). This pattern of mineral

557   homeostasis contrasts with the observations made on surface-dwelling mammals, which show

558   more pronounced bone loss with aging, especially from endocortical regions (e.g. Frost &

559   Jee, 1992; Cerroni et al., 2000; Duque & Watanabe, 2011; Bonucci & Ballanti, 2014). It has

560   been suggested that osteopenia is in part due to the inability of the skeletal system to respond

561   to mechanical loading in skeletally mature animals (Pearson & Lieberman, 2004). However,

562   studies in both animal models and humans suggest that mechanical loading minimizes the

563   extent of endosteal bone loss associated with aging (e.g. Jones et al., 1977; Bassey &

564   Ramsdale, 1994; Fehling et al., 1995; Honda et al., 2001; Lee & Lanyon, 2004; Peck & Stout,

565   2007, and references therein; Maggiano et al. 2011). Montoya-Sanhueza et al. (*in press*)

566   reported that a large part of the cortical bone of NMRs is composed of endosteal bone. It is

567   probable that endosteal surfaces maintain a high biomechanical responsiveness during

568   ontogeny and/or that the high amounts of endosteal bone formed in NMRs are more resilient

569   to resorption during ontogeny due to the increased and sustained physical activity of their

570   fossorial habits, even in captivity (Montoya-Sanhueza, 2020). Our study provides

571   histomorphological evidence to support these hypotheses: i) endosteal surfaces were still

572   active even when most modeling processes have dropped their major formative functions and

573   ii) trabeculae and endosteal margins were scarcely resorbed during long period. Thus, the low

574   bone remodeling and bone turnover of subordinates help explaining the cellular mechanisms

575   involved in the maintenance of bone structure and bone quality observed during their

576   ontogeny (Pinto et al., 2010; Carmeli-Ligati et al., 2019; Montoya-Sanhueza et al., *in press*).

577   In general, the results of this study supports a (positive) systemic regulation of the cortical

578   thickening of long bones of NMRs, where endosteal and intracortical resorption are

579   considerably down-regulated, probably because a lifestyle with sustained mechanical loading.

580   This ultimately minimizes the chances of increasing intracortical bone porosity and thus

581   reducing fracture risks during digging behavior. This may ultimately represent a functional

582   adaptation not only present in NMR, but also in other subterranean and fossorial mammals.

583

4.2   Interelement Variation in Bone Remodeling

585   The quantification of bone remodeling of all main long bones of NMRs allowed us to

586   determine the presence of interelement variation between stylopodial (humerus and femur)

587   and zeugopodial bones (ulna and tibia) (Table 3). Several lines of evidence presented in this

588   study suggest a differential pattern of bone remodeling and skeletal homeostasis among these

589   bones, which is ultimately proposed to be associated with their patterns of vascularization,

590   bone growth (modeling) and skeletal maturity.

591   The formation of secondary osteons was found more often in stylopodial bones than in

592   zeugopodial bones (Table 3). Among all bones, the humerus was the most common bone

593   developing SOs (77 in total), followed by the femur (11) and much less frequently the ulna

594   (5) and tibia (3) (Table 3). This variation is not surprising since substantial skeletal

595   heterogeneity has been previously reported in extant and extinct vertebrates, including

596   differences in bone remodeling and microstructural properties among different skeletal

597   elements (e.g. Goldstein, 1987; Amling et al., 1996; Botha & Chinsamy, 2004; Ray &

598   Chisanmy, 2004; Peck & Stout, 2007; Parfitt, 2010; Cullen et al., 2014; Martinez-Maza et al.,

599   2014; Cambra-Moo et al., 2015; Padian et al., 2016; Nacarino-Meneses et al., 2016; Bhat et

600   al., 2019; Chinsamy et al., 2020; Chinsamy, & Warburton, *in press*). However, considerable

601   variation on methodological procedures, sampling methods and taxonomic biases among

602   these studies, have greatly obscured the real nature of such patterns (see details in Cho &

603   Stout, 2011; Padian et al., 2016). For this reason, a complete overview of the causes of such

604   variations is out of the scope of the present study, and we rather focus on the most relevant

605   aspects discussed in the literature.

606   In general, interelement variation of bone remodeling has been attributed to differing

607   mechanical loading histories between bones, so that high strain magnitudes and frequencies

608   are positively correlated with increased bone remodeling (Cho & Stout, 2011; Pearson &

609   Lieberman, 2004; Cambra-Moo et al., 2015). However, in humans and many vertebrates,

610   bone remodeling also tends to be relatively accelerated in ribs, spine and pelvis, which are

611   areas with high bone turnover (Foote, 1916; Parfitt, 2002b; Cho & Stout, 2011; Currey et al.,

612   2017) and not necessarily experiencing high biomechanical strains (McFarlin et al., 2008;

613   Lad et al., 2016; Currey et al., 2017). Thus, the causes of bone remodeling are not conclusive.

614   In the case of NMRs, it is expected that forelimb bones would experience higher strains

615   (especially bending) as compared to hindlimb bones due to their direct involvement in

616   scratch-digging behavior. This would explain the fact that the cumulative amount of bone

617   remodeling is indeed higher in the forelimb (Table 3), although mostly concentrating in the

618   humerus. The actual biomechanical loading histories of these bones, especially between

619   humerus and ulna are unknown for fossorial animals, making it difficult to estimate the real

620   strains experienced during locomotion and digging behavior. Further studies assessing the

621   normal and conditioned loading strains among these bones in NMRs may help explaining the

622   relationship between mechanical load and bone remodeling.

623   Some authors have hypothesized that the lower remodeling activity of small mammals is

624   determined by their small body size and thin cortical walls (i.e. reduced bone surface), which

625   would not accommodate the cavities produced by the remodeling process, making them

626   prone to failure (Felder et al., 2017; Currey et al., 2017). Thus, the fact that Haversian

627   remodeling in NMRs occurred less frequently in smaller and slender bones (with

628   comparatively smaller cross-sectional areas) may represent an adaptation to reduce fracture

629   risk by reducing the formation of too large resorption cavities. In this sense, it is likely that

630   the reduction of bone remodeling in fossorial species such as NMRs that experience high

631   biomechanical strains throughout life may be the result of selective pressures for a less

632   variable skeletal homeostasis, particularly in the smaller bones of their skeletons.

633   Nevertheless, it is important to note that the reduced formation of SOs in these smaller bones

634   (ulna and tibia) may actually represent the lower incidence of both vascularization and

635   resorption cavities of these bones as compared to the humerus and femur (see Montoya-

636   Sanhueza et al., *in press*), rather than differences in bone size *per se.*

637   The better vascularization, high formation of resorption cavities and higher occurrence of

638   SOs in stylopodial elements (in comparison to zeugopodial elements) are all co-variants

639   associated with increased growth rates and fast bone turnover in the humerus and femur. This

640   is in agreement with that fact that most of the osteogenic activity observed in the

641   fluorochrome analysis was associated with humeri and femora (Table 2). Overall, these data

642   indicates comparatively low rates of bone turnover for the ulna and tibia and therefore a more

643   stable skeletal homeostasis for these bones as compared to the humerus and femur.

644   In developmental terms, this information suggest that zeugopodial bones may have also

645   decreased (or ceased) their main modeling (growth) functions, while stylopodial bones may

646   have still experienced some levels of bone modeling during the labeling period. This latter is

647   supported by the periosteal bone formation observed in the lateral side of the femur (Fig. 4B).

648   Some authors have proposed that the later attainment of skeletal maturity of some bones (i.e.

649   relative time of growth - heterochrony) may explain the patterns of interelement variation by

650   accumulating differential degrees of remodeling throughout life (Mulhern, 2000; Cho &

651   Stout, 2011). To explain the differences in amount of bone remodeling between the femora

652   and ribs of human archeological populations Mulhern (2000) proposed that if the femur takes

653   a longer time to mature than the rib, fewer SOs would have accumulated at any given

654   chronological age. More recently, Padian et al. (2016) suggested a similar hypothesis to

655   address the fact that small bones of large and fast growing vertebrates such as dinosaurs

656   accumulate higher levels of intracortical remodeling in comparison to large bones. Contrary

657   to our findings, these latter authors found higher levels of bone remodeling in smaller bones,

658   thus suggesting that the degree of bone remodeling in such animals is a function of different

659   growth trajectories among elements and whole-body metabolic rates, so that larger bones use

660   their energy to growth instead of developing SOs (Padian et al., 2016).

661   The analysis of epiphyseal fusion in NMRs provided important information to support the

662   hypothesis of an earlier attainment of skeletal maturity in zeugopodial bones. The pattern of

663   endochondral ossification and growth plate closure demonstrated that the ulna accumulated a

664   substantial number of cases of double fusion, having more non-growing bones as compared

665   to the other long bones of the same individual (Fig. 1A; Table S1). Certainly, this indicates

666   that the ulna fuse its epiphyses before the humerus and therefore stops growing (elongating)

667   earlier. Contrarily, the humerus showed the lowest number of epiphyseal double fusions

668   among all bones analyzed (Fig. 1A: Table S1), thus suggesting that its proximal epiphysis

669   may still be growing during late ontogeny and probably maintains a more variable and active

670   skeletal homeostasis throughout life. Regarding the hindlimb, the tibia showed only slightly

671   lower levels of double fusion than the femur (Table S1), so it appears that the hindlimb bones

672   have more equal timing of bone elongation and radial growth as compared to forelimbs, thus

673   enabling the continuation of growth for longer time as compared to the forelimb bones. At

674   this respect, Pinto et al. (2010) showed significant changes in the femoral length (FL),

675   cortical area and cortical thickness of captive individuals of NMRs ranging between 2-15

676   years old. This suggests that the femur of NMRs may continue growing in specimens older

677   than two years old. Likewise, unfused femoral epiphyses in 2 year old specimens were

678   reported by Edrey et al. (2011), thus indicating that at this age, growth plates were still active.

679   Moreover, Montoya-Sanhueza et al. (*in press*) reported that during the early postnatal

680   ontogeny of NMRs, the zeugopodial bones showed increased bone thickening (and smaller

681   medullary cavities) as compared to stylopodial bones of the same individual, thus indicating

682   that intramembranous (radial) ossification in zeugopodial elements attained maturity earlier

683   than stylopodial elements (i.e. ulna and tibia reach peak bone mass before the humerus and

684   femur). These data suggests an earlier attainment of relative skeletal maturity of distal

685   elements in NMRs.

686   Another factor associated with the increased bone turnover of stylopodial elements is the

687   development of bony protuberances. SOs in the humerus were associated with sites for

688   muscle attachment, specifically with the anterolateral side of the bone where the deltoid crest

689   develops (Montoya-Sanhueza, 2020). This region of the cortex (in bathyergids and other

690   mammals) is usually well-vascularized and exhibits high intracortical porosity during

691   ontogeny (Enlow, 1962, 1963; Montoya-Sanhueza & Chinsamy, 2017; Montoya-Sanhueza,

692   2020; Chinsamy & Warburton, *in press*; Montoya-Sanhueza et al., *in press*), thus indicating

693   that the development of SOs is directly associated with regions of high vascularization and

694   high bone turnover. Enlow (1962, 1963) described this pattern and suggested that the

695   sequential resorptive and depositional activities of remodeling serve as a mechanism for the

696   relocation of muscles and other soft tissue attachments along growing bone surfaces

697   (McFarlin et al, 2008, and references therein). The humerus of fossorial species including

698   bathyergids and other non-fossorial mammals undergoes a dynamic process of bone

699   modeling for the relocation of the deltoid and pectoral tuberosities/crests during bone growth

700   (Montoya-Sanhueza & Chinsamy, 2017; Montoya-Sanhueza, 2020; Chinsamy & Warburton,

701   *in press*). Most important, the humerus of mammals experience variable degrees of torsion

702   during its morphogenesis (Maggiano et al., 2015; Montoya-Sanhueza & Chinsamy, 2017, and

703 references therein). In this sense, Montoya-Sanhueza & Chinsamy (2018) suggested that the

704 intracortical porosity of the humerus of *B. suillus* is expected to be higher than the one

705 quantified for the femur, regardless the gender of the individual. Although we did not

706 quantify the intracortical porosity of different bones, the humerus of NMRs seems to follow a

707 similar pattern to that observed in *B. suillus*. It is likely that these morphogenetic factors

708 contribute substantially to the increased bone turnover of this element. However, because the

709 considerably reduced size of the deltoid tuberosity in NMRs in comparison to other

710 bathyergids (Montoya-Sanhueza, 2020), it is likely that this high bone turnover is rather

711 associated with the intrinsic rotation of the humerus in this species. Additionally, the femur

712 does not undergo diaphyseal rotation and does not exhibit a protuberant tuberosity, although

713 the presence of the third trochanter in its proximal region may be associated with the more

714 frequent development of SOs in comparison to the tibia, although much less frequent than the

715 humerus.

716 Consequently, there does not appear to be a single causal factor explaining our observations

717 on interelement variation. However, the pattern of vascularization and differential timing of

718 growth sequences (heterochrony) between bones may represent an important set of co-

719 variants determining the pattern of bone remodeling in NMRs and possibly in other animals

720 (Mulhern, 2000; Cho & Stout, 2011; Padian et al., 2016). Additionally, the finding of high

721 variability in the pattern of skeletal homeostasis among different elements of early mammals

722 and their ancestors (e.g. Botha & Chinsamy, 2004; Ray & Chinsamy, 2004) evidences that

723 bone remodeling and its interelement variation represent an ancestral feature among

724 therapsids, probably associated with the diverse heterochronic patterns of growth and

725 maturity of the skeletal system described for this lineage (Ray et al., 2004; Chinsamy-Turan,

726 2012b; Huttenlocker & Jennifer Botha-Brink, 2014; O'Meara & Asher, 2016).

727 This information points to the fact that the selection of bone elements for histological analysis

728 may be highly relevant for further assessments of different aspects of the bone biology of

729 vertebrates such as bone matrix maturation, early morphogenesis, skeletochronology,

730 periodic osteogenesis and biomechanical function (e.g. Cho & Stout, 2011; Padian et al.,

731 2016). This is even more pertinent when assessing different aspects of the skeletal

732 homeostasis such as sex-related bone loss, age-related bone loss and reproduction-related

733 mineral mobilization (e.g. Parfitt, 2010; Doherty et al., 2015).

734   ## 4.3   Bone Remodeling in Breeders: the Effects of Reproduction

735   High bone remodeling was detected in some female breeders, although other females did not

736   present considerable changes in their bone microstructure (Fig. 5). This indicated a high

737   variation in bone remodeling among breeders. Pinto et al. (2010) briefly mentioned

738   endocortical bone resorption in late pregnancy and during lactation in NMRs, although they

739   did not provide histomorphological evidence for this process. Dengler-Crish & Catania

740   (2009) reported reproduction-related bone formation during spine elongation at the onset of

741   reproductive activity and pregnancy. These studies suggest a high level of variation in

742   skeletal homeostasis in reproductive NMRs, which is probably associated with the multiphase

743   nature of female's reproductive cycle which involves pregnancy, lactation and postlactation.

744   Mammalian females are known to undergo marked fluctuations of their skeletal homeostasis,

745   such as high mineral imbalances and skeletal deterioration, especially during lactation so that

746   they can meet the needs of fetal development (Redd et al., 1984; Kovacs & Kronenberg,

747   1997; Kovacs, 2001, 2005; Vajda et al. 2001; Cerroni et al., 2003; Miller & Bowman, 2004).

748   These effects are augmented when females experience food resource limitation. Experimental

749   studies have reported how Sprague–Dawley rats on a low-calcium diet have increased

750   intracortical remodeling and developed a great number of SOs during lactation as compared

751   to controls with normal diets (Ruth, 1953; Ross & Sumner, 2017). These data demonstrate a

752   clear increase in bone dynamics (bone turnover) associated with reproductive cycles and

753   indicates that the processes of gain and loss of mineral content from female skeletons are

754   temporally regulated. For example, anabolic activity has been reported during some phases of

755   reproduction in mammals, specifically during postlactation (Vajda et al. 2001; Miller &

756   Bowman, 2004). Thus, the variation in the remodeling pattern observed among breeders in

757   this study may be associated with the specific reproductive stages that these females

758   experienced. Because NMR queens often become pregnant again during lactation (Jarvis,

759   1991) they show a minimal postlactation period, which is usually destined for skeletal

760   recuperation (Miller & Bowman, 2004). However, Dengler-Crish & Catania (2009)

761   suggested that the anabolic effects of new pregnancies may lessen the impact of bone loss

762   that commonly occurs in lactating females. Unfortunately, no information on the specific

763   reproductive stages that the breeders of this study were experiencing is available.

764   A similar generalized catabolic activity in the appendicular skeleton of females of the solitary

765   *B. suillus* have been reported, most likely as an effect of reproduction (Montoya-Sanhueza &

766   Chinsamy, 2017). This demonstrate that NMRs and African mole-rats may share a similar

767   mechanism of mineral mobilization regulated by sex steroids during reproduction as

768   compared to other mammals (Dengler-Crish & Catania, 2009; Montoya-Sanhueza &

769   Chinsamy, 2018). Nevertheless, additional studies assessing the extension and magnitude of

770   different reproductive phases, as well as its effects on the female skeleton are further

771   required, especially considering that female breeders in NMRs can experience successive

772   pregnancies over a short period.

773   Overall, it is likely that the increased remodeling observed in female breeders is associated

774   with the increased metabolism that females experience during reproduction. Urison &

775   Buffenstein (1995) showed that the metabolic rate of pregnant NMRs is 1.4-fold higher as

776   compared to subordinate individuals. Similar findings have been reported for the female

777   breeders of the social Ansell's mole-rat, *F. anselli* (Schielke et al., 2017). In this sense,

778   increased metabolic rates may trigger not only skeletal anabolism but bone remodeling, thus

779   increasing the levels of bone turnover and mineral mobilization for quick release of calcium

780   destined for pup development. Likewise, the scarce bone remodeling observed in subordinate

781   NMRs may also be associated with their generalized lower metabolic rates (Montoya-

782   Sanhueza et al., *in press*). This would be in agreement with recent evidence showing that

783   bone tissue matrices in NMRs are predominantly characterized by slowly deposited bone

784   tissues and scarce vascularization (Montoya-Sanhueza & Chinsamy, 2016; Carmeli-Ligati et

785   al., 2019; Montoya-Sanhueza et al. *in press*).

786

787   ## 5.   CONCLUSIONS

788   In general, NMRs exhibited low levels of bone resorption and bone remodeling, most likely

789   linked to their low vascularization, low metabolic rates and generalized slow growth rates.

790   The reduced activity of this process represents one of the cellular-level mechanisms

791   explaining the maintenance of high bone quality and bone structure during the ontogeny of

792   NMRs. The low remodeling activity seems to represent a generalized process in AMs and

793   probably other subterranean and fossorial mammals. Bone remodeling was mainly observed

794   in stylopodial (larger) bones as compared to zeugopodial (smaller) bones, thus suggesting a

795   higher degree of bone turnover in these larger elements. Zeugopodial bones appeared to have

796   attained maturity before stylopodial elements, thus showing reduced cellular activity and

797   bone remodeling in adults. It is suggested that higher levels of vascularization, longer

798   modeling activity (delayed skeletal maturity) and the development of bone tuberosities of

799   stylopodial bones are important determinants of the degree of bone remodeling. Nevertheless,

800   bone remodeling increased in some productive females, thus following a similar pattern to

801   that found in other mammals during reproduction. This was associated with a higher

802   metabolism of breeders as compared to subordinates, so that increments in metabolic rate are

803   linked to increased remodeling activity. Consequently, it is suggested that bone remodeling in

804   NMRs appeared to be associated with activities involving high metabolism, such as

805   relocation of diaphyseal structures and reproduction. This information represents an

806   important aspect of the skeletal homeostasis of NMRs, which help understanding the tissue-

807   and cellular-level processes involved in the maintenance of high bone quality during a

808   species with prolonged lifespan. Moreover, based on histomorphological comparisons with

809   other mammals and extinct vertebrates such as non-mammalian therapsids, the lineage that

810   gave rise to mammals, it was observed that both the endocortical compartmentalization of

811   bone remodeling and its interelement variability represent ancestral features, probably

812   associated with the early evolution of differential patterns of bone (re)modeling among these

813   extinct taxa.

814

829

Author contribution

831   GMS and AC designed the study; AC supervised GMS's doctoral thesis and supported the
832   experimental procedures; NB supported the experimental procedures; NB and CDC provided NMR
833   specimens; MO and GMS quantified data and carried out bone labeling procedures; GMS, analyzed
834   data, prepared the manuscript, created figures, acquired microscopy images; all authors read, edited
835   and approved the manuscript.

836

Declaration of competing interest

The authors declare no conflict of interest.

References

Allen M, Burr D. 2014. Bone Modeling and Remodeling (Ch. 4). In: Basic and Applied Bone Biology (Eds DB Burr, M Allen), pp. 373. Academic Press, Elsevier, London.

Amling M, Herden S, Posl M, Hahn M, Ritzel H, Delling G. 1996. Heterogeneity of the skeleton: Comparison of the trabecular microarchitecture of the spine, the iliac crest, the femur, and the calcaneus. J Biomech 20:36–45.

Amprino, R. 1948. A contribution to the functional meaning of the substitution of primary by secondary bone tissue. Acta. Anatomica, 5, part, 3: 291-300.

Andersen TL, Abdelgawad ME, Kristensen HB, et al. 2013. Understanding coupling between bone resorption and formation: are reversal cells the missing link?. Am J Pathol. ;183(1):235-246.

Bassey EJ, Ramsdale SJ. 1994. Increase in femoral bone density in young women following high impact exercise. Osteoporos Int 4:72–75.

Bhat SM, Chinsamy A, Parkington J. 2019. Long bone histology of *Chersina angulata*: Interelement variation and life history data. Journal of Morphology; 1–19.

Bennett NC, Jarvis J, Aguilar GH, Mcdaid EJ. 1991. Growth and development in six species of African mole-rats (Rodentia: Bathyergidae). Journal of Zoology 225: 13–26.

Bonucci E, Ballanti P. 2014. Osteoporosis-bone remodeling and animal models. Toxicol Pathol.; 42(6):957-69

Botha-Brink J, Angielczyk KD. 2010. Do extraordinarily high growth rates in Permo-Triassic dicynodonts (Therapsida, Anomodontia) explain their success before and after the end-Permian extinction? Zool. J. Linn. Soc. 160, 341–365. (doi:10.1111/j.1096-3642.2009.00601.x)

Botha, J., Chinsamy, A. 2004. Growth and life habits of the Triassic cynodont *Trirachodon*, inferred from bone histology. Acta Palaeontologica Polonica 49 (4): 619–627.

Braude, S., Holtze, S., Begall, S., Brenmoehl, J., Burda, H., Dammann, P., del Marmol, D., Gorshkova, E., Henning, Y., Hoeflich, A., Höhn, A., Jung, T., Hamo, D., Sahm, A., Shebzukhov, Y., Šumbera, R., Miwa, S., Vyssokikh, M.Y., von Zglinicki, T., Averina, O. Hildebrandt, T.B. 2020. Surprisingly long survival of premature conclusions about naked mole-rat biology. Biol Rev. doi: 10.1111/brv.12660

Bromage TG, Goldman HM, McFarlin SC J. Warshaw, A. Boyde, C. M. Riggs. 2003. Circularly polarized light standards for investigations of collagen fiber orientation in bone. *Anatomical record. Part B, New anatomist* **274**, 157–68.

Buffenstein, R, KN Lewis, PA Gibney, V Narayan, KM Grimes, M Smith, TD Lin, HM Brown-Borg. 2020. Probing Pedomorphy and Prolonged Lifespan in Naked Mole-Rats and Dwarf Mice. Physiology, 35:2, 96-111.

886

887 **Buffenstein, R, T. Park, M. Hanes, J.E. Artwohl. 2012.** Naked mole rat. In: M.A. Suckow, K.A.
888 Stevens, R.P. Wilson (Eds.), The Laboratory Rabbit, Guinea Pig, Hamster, and Other Rodents., Elsevier,
889 pp. 1055-1074.

891 **Buffenstein R, Yahav, 1991.** Is the naked mole-rat, *Heterocephalus glaber*, a poikilothermic or poorly
892 thermoregulating endothermic mammal? *J Therm Biol.* 16:227–232.

894 **Cambra-Moo, O., Nacarino-Meneses, C., Díaz-Güemes, I., Enciso, S., García Gil, O., Llorente**
895 **Rodríguez, L., Rodríguez Barbero, M.Á., de Aza, A.H., González Martín, A., 2015.** Multidisciplinary
896 characterization of the long-bone cortex growth patterns through sheep's ontogeny. J. Struct. Biol. 191,
897 1–9.

899 **Cambra-Moo, O., Nacarino Meneses, C., Rodríguez Barbero, M.A., García Gil, O., Rascón Pérez,**
900 **J., Rello Varona, S., D'Angelo, M., Campo Martín, M., González Martín, A., 2014.** An approach to
901 the histomorphological and histochemical variations of the humerus cortical bone through human
902 ontogeny. J. Anat. 224 (6), 636–646.

904 **Castanet J, Croci S, Aujard F, M. Perret, J. Cubo, and E. de Margerie. 2004.** Lines of arrested growth
905 in bone and age estimation in a small primate: *Microcebus murinus. Journal of zoology of london* **263**, 31–
906 39.

908 **Carmeli-Ligati S, Anna Shipova, Maïtena Dumont, Susanne Holtz, Thomas Hildebrandt, Ron**
909 **Shahar. 2019** The structure, composition and mechanical properties of the skeleton of the naked mole-
910 rat (*Heterocephalus glaber*). Bone (128), 115035.

912 **Cerroni AM, Tomlinson GA, Turnquist JE, Grynpas MD. 2000.** Bone mineral density, osteopenia,
913 and osteoporosis in the rhesus Macaques of Cayo Santiago. American Journal of Physical Anthropology
914 113: 389–410.

916 **Chinsamy, A, D. Angst, A. Canoville, U.B. Göhlich. 2020.** Bone histology yields insights into the
917 biology of the extinct elephant birds (Aepyornithidae) from Madagascar Biol. J. Linn. Soc., 130 (2020),
918 pp. 268-295 .

920 **Chinsamy, A, Warburton, NM. *In Press*.** Ontogenetic growth and the development of a unique
921 fibrocartilage entheses in *Macropus fuliginosus*. Zoology (In Press).
922 https://doi.org/10.1016/j.zool.2020.125860

924 **Chinsamy-Turan A. 2012(a)**. The microstructure of bones and teeth of nonmammalian therapsids. In:
925 Chinsamy-Turan A, ed. Forerunners of mammals: radiation, histology, biology. Bloomington and
926 Indianapolis: Indiana University Press, 65–88.

928 **Chinsamy-Turan A. 2012(b)**. Forerunners of mammals: radiation, histology, biology. Bloomington and
929 Indianapolis: Indiana University Press.

931 **Chinsamy A, Hurum J. 2006.** Bone microstructure and growth patterns of early mammals. *Acta*
932 *Palaeontologica Polonica* **51**, 325–338.

934 **Chinsamy-Turan A. 2005**. The Microstructure of Dinosaur Bone. Deciphering Biology with Fine-Scale
935 Techniques. Baltimore, Maryland: The Johns Hopkins University Press.

937 **Cho H, Stout SD. 2011.** Age-associated bone loss and intraskeletal variability in the Imperial Romans. J
938 Anthropol Sci.; 89:109-25

940 **Cullen, T.M., Evans, D.C., Ryan, M.J. et al. 2014.** Osteohistological variation in growth marks and
941 osteocyte lacunar density in a theropod dinosaur (Coelurosauria: Ornithomimidae). BMC Evol Biol 14,
942 231.

Currey, M.N. Dean, R. Shahar. 2017. Revisiting the links between bone remodeling and osteocytes: insights from across phyla, Biol. Rev. Camb. Philos. Soc. 92: 1702–1719.

Currey J. 2002. Bone. Structure and Mechanics. Princeton University Press, Oxfordshire, UK.

Dammann P, Burda H. 2007. Senescence patterns in African mole-rats (Bathyergidae, Rodentia). In: Begall S, In: Burda H., In: Schleich C, eds. Subterranean Rodents : News from Underground. Heiderberg, Germany : Springer-Verlag, 251-263.

Dengler-Crish C, Catania KC. 2009. Cessation of Reproduction-Related Spine Elongation After Multiple Breeding Cycles in Female Naked Mole-Rats. Anatomical Record (Hoboken) 292: 131–137.

Dengler-crish CM, Catania KC. 2007. Phenotypic plasticity in female naked mole-rats after removal from reproductive suppression. Journal of Experimental Biology 210: 4351–4358.

Doherty, A. H., Ghalambor, C. K. & Donahue, S. W. 2015. Evolutionary physiology of bone: bone metabolism in changing environments. Physiology 30, 17-29.

Duque G, Watanabe K. 2011. *Osteoporosis Research. Animal Models* (G Duque and K Watanabe, Eds.). London: Springer London.

Edrey YH, Park TJ, Kang H, Biney A. Buffenstein R. 2011. Endocrine function and neurobiology of the longest-living rodent, the naked molerat. *Exp Gerontol*, 46:116–123.

Enlow DH. 1969. The Bone of Reptiles. In: Biology of the Reptilia Vol. 1 Morphology A (ed C Gans), pp. 373. Academic Press, London.

Enlow DH. 1963. Principles of Bone Remodeling. An Account of Post-natal Growth and Remodeling Processes in Long Bones and the Mandible. Springfield, IL: Charles C. Thomas.

Enlow, D.H. 1962. Functions of the haversian system. Am. J. Anat., 110: 269-305.

Enlow D, Brown S. 1958. A comparative histological study of fossil and recent bone tissues. Part III. The Texas Journal of Science 10: 187–230.

Enlow, D.H., Brown, S.O., 1956. A comparative histological study of fossiland recent bone tissues. Part I. Tex. J. Sci. 8, 405–443.

Farnum, C. E. 2007. Postnatal growth of fins and limbs through endochondral ossification; pp. 118–151 in B. K. Hall (ed.), Fins into Limbs: Evolution, Development, and Transformation. University Chicago Press, Chicago (Illinois) and London.

Fehling PC, Alekel L, Clasey J, Rector A, Stillman RJ. 1995. A comparison of bone mineral densities among female athletes in impact loading and active loading sports. Bone 17:205–210.

Felder AA, Phillips C, Cornish H, Cooke M, Hutchinson JR, Doube M. Secondary osteons scale allometrically in mammalian humerus and femur. R Soc Open Sci. 2017;4(11):170431. Published 2017 Nov 8. doi:10.1098/rsos.170431

Foote, J. S. 1916. A Contribution to the Comparative Histology of the Femur. Aleš Hrdlička Ed. Smithsonian Institution. 246 pp.

Forwood MR, Parker AW. 1986. Effects of exercise on bone morphology: Vascular channels studied in the rat tibia. Acta Orthopaedica 57, 204–207.

998   **Francillon-Vieillot H, de Buffrénil V, Castanet J. 1990.** Microstructures and mineralization of
999   vertebrate skeletal tissues. In: *Skeletal biomineralizations: patterns, processes and evolutionary trends*
1000   (ed Carter J), pp. 471–530. Van Nostrand Reinhold, New York.
1001
1002   **Frost HM, Jee WS. 1992.** On the rat model of human osteopenias and osteoporoses. Bone and Mineral
1003   18, 227–236.
1004
1005   **Frost HM. 1987(a).** Bone "mass" and the "mechanostat": a proposal. *The Anatomical record* **219**, 1–9.
1006
1007   **Frost H.M. 1987(b).** Secondary osteon population densities: an algorithm for estimating the missing
1008   osteons. Yearb. Phys. Anthropol., 30:239-254.
1009
1010   **Frost HM. 1969.** Tetracycline-based histological analysis of bone remodeling. *Calcified tissue research* **3**,
1011   211–237.
1012
1013   **Geiger, M., LAB. Wilson, L. Costeur, R. Sánchez, MR Sánchez-Villagra. 2013.** Diversity and body
1014   size in giant caviomorphs (Rodentia) from the northern Neotropics—a study of femoral variation.
1015   Journal of Vertebrate Paleontology 33:1449–1456.
1016
1017   **Goldman, H. M., S. C. McFarlin, D. M. L. Cooper, C. D. L. Thomas, J. G. Clement. 2009.**
1018   Ontogenetic patterning of cortical bone microstructure and geometry at the human mid-shaft femur.
1019   *Anatomical record* **292**, 48–64.
1020
1021   **Goldstein SA. 1987.** The mechanical properties of trabecular bone: Dependence on anatomic location
1022   and function. J Biomech 20:1055–1061.
1023
1024   **Havill LM, Allen MR, Harris JA, Levine SM, Coan HB, Mahaney MC, Nicolella DP. 2013.**
1025   Intracortical bone remodeling variation shows strong genetic effects. Calcif Tissue Int.; 93(5):472-80.
1026
1027   **Henry EC, Dengler-Crish CM, Catania KC. 2007.** Growing out of a caste - reproduction and the
1028   making of the queen mole-rat. Journal of Experimental Biology 210: 261–268.
1029
1030   **Hillier, M.L. Bell, L.S. 2007.** Differentiating Human Bone from Animal Bone: A Review of Histological
1031   Methods. Journal of Forensic Sciences, 52: 249-263.
1032
1033   **Holtze, S., Braude, S., Lemma, A., Koch, R., Morhart, M., Szafranski, K., Platzer, M., Alemayehu,**
1034   **F., Goeritz, F., Hildebrandt, T.B., 2018.** The microenvironment of naked mole-rat burrows in East
1035   Africa. Afr. J. Ecol. 56, 279–289.
1036
1037   **Honda A, Umemura Y, Nagasawa S. 2001.** Effect of high-impact and low-repetition training on bones
1038   in ovariectomized rats. J. Bone Miner Res 16:1688–1693.
1039
1040   **Hood, W. R., Kessler, D. S., Oftedal, O. T. 2014.** Milk composition and lactation strategy of a eusocial
1041   mammal, the naked mole-rat. Journal of Zoology, 293(2), 108–118.
1042
1043   **Huttenlocker AK, J Botha-Brink (2014)** Bone microstructure and the evolution of growth patterns in
1044   Permo- Triassic therocephalians (Amniota, Therapsida) of South Africa. PeerJ 2:e325; DOI
1045   10.7717/peerj.325.
1046
1047   **Jarvis JUM., PW. Sherman. 2002.** *Heterocephalus glaber.* Mammalian Species, No. 706: 1-9.
1048
1049   **Jarvis, J. 1991.** Reproduction of Naked Mole-rats. In: The Biology of the Naked mole-rat. (Ed. by P.W.
1050   Sherman, J.U.M. Jarvis and R.D. Alexander), pp. 384-425. Princeton University Press, Princeton, New
1051   Jersey.
1052
1053   **Jaworski, Z. F. G. 1992.** Haversian systems and Haversian bone. In Bone, Volume 4: Bone Metabolism
1054   and Mineralization (B. K. Hall, ed.), pp. 21–45. CRC Press, Boca Raton, FL.

1055
1056 **Jones HH, Priest JD, Hayes WC, Tichenor CC, Nagel DA. 1977.** Humeral hypertrophy in response to
1057 exercise. J Bone Joint Surg 59:204–208.
1058
1059 **Jowsey J. 1966.** Studies of Haversian systems in man and some animals. J Anat.; 100(4):857-864.
1060
1061 **Kearns AE, Khosla S, Kostenuik PJ. 2008.** Receptor activator of nuclear factor kappaB ligand and
1062 osteoprotegerin regulation of bone remodeling in health and disease. Endocr Rev. 2008;29(2):155-192.
1063
1064 **Kim JN, Lee JY, Shin KJ, Gil YC, Koh KS, Song WC. 2015.** Haversian system of compact bone and
1065 comparison between endosteal and periosteal sides using three-dimensional reconstruction in rat. Anat
1066 Cell Biol.;48(4):258-261.
1067
1068 **Kovacs CS. 2001.** Calcium and bone metabolism during pregnancy and lactation. Journal of Clinical
1069 Endocrinology and Metabolism 96: 105–18.
1070
1071 **Kovacs CS. 2005.** Calcium and Bone Metabolism During Pregnancy and Lactation. 10: 105–118.
1072
1073 **Kovacs C, Kronenberg H. 1997.** Maternal-fetal calcium and bone metabolism during pregnancy,
1074 puerperium, and lactation. Endocrine Rev. 18: 832–872.
1075
1076 **Lad, S.E., Daegling, D.J. McGraw, W.S. (2016)** Bone remodeling is reduced in high stress regions of
1077 the cercopithecoid mandible. Am. J. Phys. Anthropol., 161: 426-435.
1078
1079 **Lee KCL, Lanyon LE. 2004.** Mechanical loading influences bone mass through estrogen receptor.
1080 Osteoporos Int 15:42–50.
1081
1082 **Locke M. 2004.** Structure of long bones in mammals. J Morphol 262, 546–565.
1083
1084 **Maggiano, I.S., C.M. Maggiano, J.G. Clement, C.D.L. Thomas, Y. Carter, D.M.L. Cooper. 2016.**
1085 Three-dimensional reconstruction of Haversian systems in human cortical bone using synchrotron
1086 radiation-based micro-CT: morphology and quantification of branching and transverse connections
1087 across age. Journal of Anatomy, 228, pp. 719-732
1088
1089 **Maggiano IS, Maggiano CM, Tiesler VG, et al. (2015)** Drifting diaphyses: asymmetry in diametric
1090 growth and adaptation along the humeral and femoral length. Anat Rec 289(10), 1689–1699.
1091
1092 **Maggiano IS, Maggiano CM, Tiesler V, Kierdorf H, Stout SD, Schultz M. 2011.** A distinct region of
1093 microarchitectural variation in femoral compact bone: Histomorphology of the endosteal lamellar
1094 pocket. Int J Osteoarch 21:743–750.
1095
1096 **Martin RB, Burr DB, Sharkey N. 1998.** Skeletal Tissue Mechanics. New York: Springer-Verlag.
1097
1098 **Martinez-Maza C, Alberdi MT, Nieto-Diaz M, Prado JL. 2014.** Life-History Traits of the Miocene
1099 *Hipparion concudense* (Spain) Inferred from Bone Histological Structure. PLoS ONE 9(8): e103708.
1100
1101 **McFarlin, S.C., Terranova, C.J., Zihlman, A.L., Enlow, D.H. and Bromage, T.G. 2008.** Regional
1102 variability in secondary remodeling within long bone cortices of catarrhine primates: the influence of
1103 bone growth history. Journal of Anatomy, 213: 308-324.
1104
1105 **Miller SC, Bowman BM. 2004.** Rapid improvements in cortical bone dynamics and structure after
1106 lactation in established breeder rats. Anat Rec A Discov Mol Cell Evol Biol 276:143–149.
1107
1108 **Miller, S. C., Shupe, J. G., Redd, E. H., Miller, M. A., Omura, T. H. 1986.** Changes in bone mineral
1109 and bone formation rates during pregnancy and lactation in rats. Bone 7:283–287.
1110

Montoya-Sanhueza, G, NC. Bennett, MK. Oosthuizen, CM. Dengler-Crish, A Chinsamy. (in press) Long bone histomorphogenesis of the naked mole-rat: histodiversity and intraspecific variation. Journal of Anatomy.

Montoya-Sanhueza, G. 2020. Functional Anatomy, Osteogenesis and Bone Microstructure of the Appendicular System of African Mole-Rats (Rodentia: Ctenohystrica: Bathyergidae). PhD Thesis. Submitted to the Department of Biological Sciences, University of Cape Town, South Africa. 268 p.

Montoya-Sanhueza G & Chinsamy A. 2018. Cortical bone adaptation and mineral mobilization in the subterranean mammal *Bathyergus suillus* (Rodentia: Bathyergidae): effects of age and sex. PeerJ 6:e4944.

Montoya-Sanhueza, G & A. Chinsamy. 2017. Long bone histology of the subterranean rodent *Bathyergus suillus* (Bathyergidae): ontogenetic pattern of cortical bone thickening. Journal of Anatomy, 230:203-233.

Montoya-Sanhueza, G & Chinsamy A. 2016. Bone microstructure of two highly specialised subterranean rodents: *Bathyergus suillus* and *Heterocephalus glaber* (Bathyergidae). Biennial Conference Palaeontological Society of Southern Africa (PSSA). Abstract book. Stellenbosch, South Africa, 45.

Montoya-Sanhueza, G. 2010. Diferencias microestructurales del hueso femoral en Abrothrix longipilis (Cricetidae, Sigmodontinae) en un gradiente de altitud: Una aproximación preliminar. Tesis de Título. Universidad de Concepcion. Chile. 56 pp.

Mori S, Burr DB. Increased intracortical remodeling following fatigue damage. Bone. 1993;14(2):103-109.

Mulhern DM. 2000. Rib remodeling dynamics in a skeletal population from Kulubnarti, Nubia. Am J Phys Anthropol.;111(4):519-30.

Nacarino-Meneses C, Jordana X, Kohler M. Histological variability in the limb bones of the Asiatic wild ass and its significance for life history inferences. PeerJ. 2016; 4: e2580.

O'Connor TP, Lee A, Jarvis J, Buffenstein R. 2002. Prolonged longevity in naked mole-rats: age-related changes in metabolism, body composition and gastrointestinal function. Comparative Biochemistry and Physiology. Part A, Molecular & Integrative Physiology, 133(3), 835–42.

O'Riain, M. J. 1996. Pup Ontogeny and Factors Influencing Behavioural and Morphological Variation in Naked Mole-Rats, *Heterocephalus glaber* (Rodentia, Bathyergidae). University of Cape Town.

Padian K, Werning S, Horner JR. 2016. A hypothesis of differential secondary bone formation in dinosaurs. Comptes Rendus Palevol 15, 40–48.

Patterson BD, Upham NS. 2014. A newly recognized family from the Horn of Africa, the Heterocephalidae (Rodentia: Ctenohystrica). Zoological Journal of the Linnean Society 172: 942–963.

Parfitt AM. **2010.** Skeletal Heterogeneity and the Purposes of Bone Remodeling: Implications for the Understanding of Osteoporosis. In: *Fundamentals of Osteoporosis* (eds R Marcus, D Feldman, D Nelson, C Rosen), pp. 537. Academic Press, Elsevier, London.

Parfitt AM. 2003. Misconceptions (3): calcium leaves bone only by resorption and enters only by formation. Bone, 33: 259–263.

Parfitt, A. M. 2002(a). Misconceptions (1): Epiphyseal Fusion Causes Cessation of Growth. Bone, 30:337–339.

1167   **Parfitt, A. M. 2002(b).** Misconceptions (2): Turnover Is Always Higher in Cancellous Than in Cortical
1168   Bone. Bone Vol. 30(6):807–809.
1169
1170   **Pearson OM, Lieberman DE. 2004.** The aging of Wolff 's "law": Ontogeny and responses to
1171   mechanical loading cortical bone. Am J Phys Anthropol 39:63–99.
1172
1173   **Peck J.J., Stout S.D. 2007.** Intraskeletal variability in bone mass. Am. J. Phys. Anthropol.,
1174   132:89-97.
1175
1176   **Piemontese, M., M. Almeida, A.G. Robling, H.-N. Kim, J. Xiong, J.D. Thostenson, R.S. Weinstein,**
1177   **S.C. Manolagas, C.A. O'Brien, R.L. Jilka. 2017.** Old age causes de novo intracortical bone remodeling
1178   and porosity in mice. JCI Insight, 2: 1-18.
1179
1180   **Pinto, M., K. J. Jepsen, C. J. Terranova, R. Buffenstein. 2010.** Lack of sexual dimorphism in femora
1181   of the eusocial and hypogonadic naked mole-rat: A novel animal model for the study of delayed puberty
1182   on the skeletal system. *Bone*, 46:112–120.
1183
1184   **Rabey KN, Green DJ, Taylor AB, et al. 2015.** Locomotor activity influences muscle architecture and
1185   bone growth but not muscle attachment site morphology. J Hum Evol 78, 91–102.
1186
1187   **Ray, S., Botha, J., Chinsamy, A. 2004.** Bone histology and growth patterns of some nonmammalian
1188   therapsids. J. Vert. Paleontol. 24, 634–648.
1189
1190   **Redd EH, Miller SC, Jee WSS. 1984.** Changes in endochondral bone elongation rates during pregnancy
1191   and lactation. Calcif Tissue Int; 36:697–701.
1192
1193   **Ricqlès A de, Meunier FJ, Castanet J, Francillon-Vieillot H. 1991.** Comparative microstructure of
1194   bone. In: Hall BK, ed. Bone Matrix and Bone Specific Products. Boca Raton: CRC Press, 1–78.
1195
1196   **Roach, H. I., Mehta, G., Oreffo, R. O. C., Clarke, N. M. P., & Cooper, C. 2003.** Temporal Analysis of
1197   Rat Growth Plates: Cessation of Growth with Age Despite Presence of a Physis. Journal of
1198   Histochemistry & Cytochemistry, 51(3), 373–383.
1199
1200   **Ross RD, Sumner DR**. 2017. Bone Matrix Maturation in a Rat Model of Intra-Cortical Bone Remodeling
1201   [published correction appears in Calcif Tissue Int. Apr 29;:]. Calcif Tissue Int. 2017;101(2):193-203.
1202
1203   **Ruth EB. 1953.** Bone studies. II. An experimental study of the haversian-type vascular channels. The
1204   American journal of anatomy 93: 429–455.
1205
1206   **Schielke, C.K.M., Burda, H., Henning, Y., Okrouhlík, J., Begall, S., 2017.** Higher resting metabolic
1207   rate in long-lived breeding Ansell's mole-rats (Fukomys anselli). Front. Zool. 14, 45.
1208
1209   **Seeman, E., 2008.** Modeling and remodeling: the cellular machinery responsible for the gain and loss
1210   of bone's material and structural strength. Chapter 1 In: Bilezikian, J.P., Raisz, L.G., Martin, T.J. (Eds.),
1211   Principles of Bone Biology, third edition. Academic Press, San Diego, pp. 1–28.
1212
1213   **Shelton CD, Sander PM. 2017.** Long bone histology of *Ophiacodon* reveals the geologically earliest
1214   occurrence of fibrolamellar bone in the mammalian stem lineage. C. R. Palevol. 16, 397–424. (doi:10.
1215   1016/j.crpv.2017.02.002).
1216
1217   **Singh, I., E. Tonna, C. Gandel. 1974.** A comparative histological study of mammalian bone. Journal of
1218   Morphology 144:421–437.
1219
1220   **Singh, IJ., DL. Gunberg, 1971.** Quantitative histology of changes with age in rat bone cortex. J.
1221   Morphol. 133, 241-252.
1222

1223   **Sissons, H., G. Kelman, G. Marotti. 1984.** Mechanisms of Bone Resorption in Calcium-Deficient Rats.
1224   Calcified Tissue International 36:711–721.
1225
1226   **Sherman PW, Jarvis JUM. 2002.** Extraordinary life spans of naked mole-rats (*Heterocephalus glaber*).
1227   Journal of Zoology 258: 307–311.
1228
1229   **Sherman, PW., Jarvis, J. U. M. Braude, S. 1992.** Naked mole-rats. Scientific American 267, 72–78.
1230
1231   **Straehl FR, Scheyer TM, Forasiepi AM, MacPhee RD, Sánchez-Villagra MR. 2013.** Evolutionary
1232   patterns of bone histology and bone compactness in xenarthran mammal long bones. *PloS one* **8**,
1233   e69275.
1234
1235   **Šumbera, 2019.** Thermal biology of a strictly subterranean mammalian family, the African mole-rats
1236   (Bathyergidae, Rodentia) - a review. *Journal of Thermal Biology*, 79:166-189.
1237
1238   **Thomas, C.D.L., Feik, S.A. and Clement, J.G. 2005.** Regional variation of intracortical porosity in the
1239   midshaft of the human femur: age and sex differences. Journal of Anatomy, 206: 115-125.
1240
1241   **Upham, N., Patterson, B.D. 2015.** Evolution of caviomorph rodents: a complete phylogeny and
1242   timetree for living genera, in: Vassallo, A.I., Antenucci, D. (Eds.), Biology of Caviomorph Rodents:
1243   Diversity and Evolution. SAREM Series A, Buenos Aires, pp. 63–120.
1244
1245   **Urison, N., Buffenstein, R., 1995.** Metabolic and body temperature changes during pregnancy and
1246   lactation in the naked mole-rat (*Heterocephalus glaber*). Physiol. Zool. 68, 402–420.
1247
1248   **Vajda EG, Bowman BM, Miller SC. 2001.** Cancellous and cortical bone mechanical properties and
1249   tissue dynamics during pregnancy, lactation, and postlactation in the rat. Biol Reprod. Sep;65(3):689-95.
1250
1251   **Vajda EG, Kneissel M, Muggenburg B, Miller SC. 1999.** Increased intracortical bone remodeling
1252   during lactation in beagle dogs. Biol Reprod; 61:1439–1444.
1253
1254   **Warshaw J (2008)** Comparative primate bone microstructure: records of life history, function, and
1255   phylogeny. In: Mammalian Evolutionary Morphology. A Tribute to Frederick S. Szalay. (eds Sargis E,
1256   Dagosto M), pp. 440, Vertebrate Paleobiology and Paleoanthropology Series, Netherlands: Springer.
1257
1258   **Zelová, J., Šumbera, R., Sedláček, F., Burda, H., 2007.** Energetics in a solitary subterranean rodent,
1259   the silvery mole-rat, *Heliophobius argenteocinereus* and allometry of RMR in African mole-rats
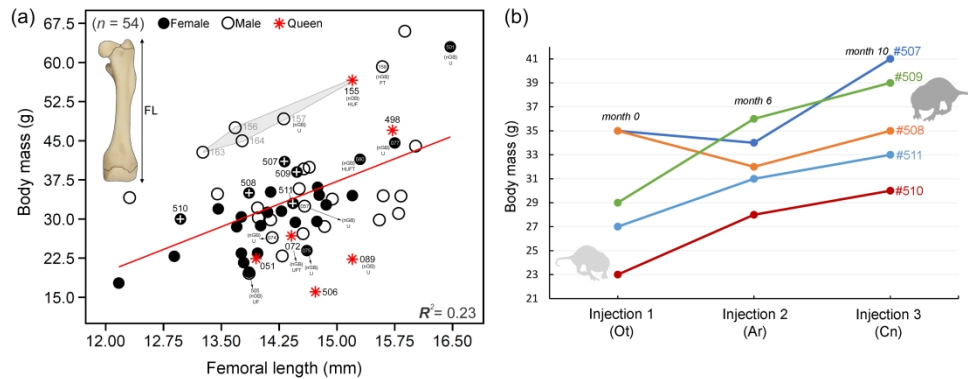1260   (Bathyergidae). Comp. Biochem. Physiol. -Mol. Integr. Physiol. 147, 412–419.
1261

Figure 1. Morphological features of adult naked mole-rats. A) Linear relationship between femoral length (FL) and body mass (BM) including non-reproductive (subordinate) individuals and female breeders (queens). Females injected with fluorochromes (#506-511) are indicated with a (+) symbol. Specimens of known-age (#155-164, between 2-3 years) are enclosed within a polygon. The bones of the individuals showing double fusion of epiphyses are also indicated; non-growing bone (nGB). Ordinary least square (OLS) parameters: R2 = 0.23, Slope = 5.795, Intercept = -49.72 (n = 54). B) Graph showing the changes in BM during the ~10 month in vivo bone labeling period. See the details of the fluorochrome experiment in Table 2. Abbreviations: alizarin red (Ar), calcein (Cn), femur (F), humerus (H), oxytetracycline (Ot), ulna (U), tibia (T).
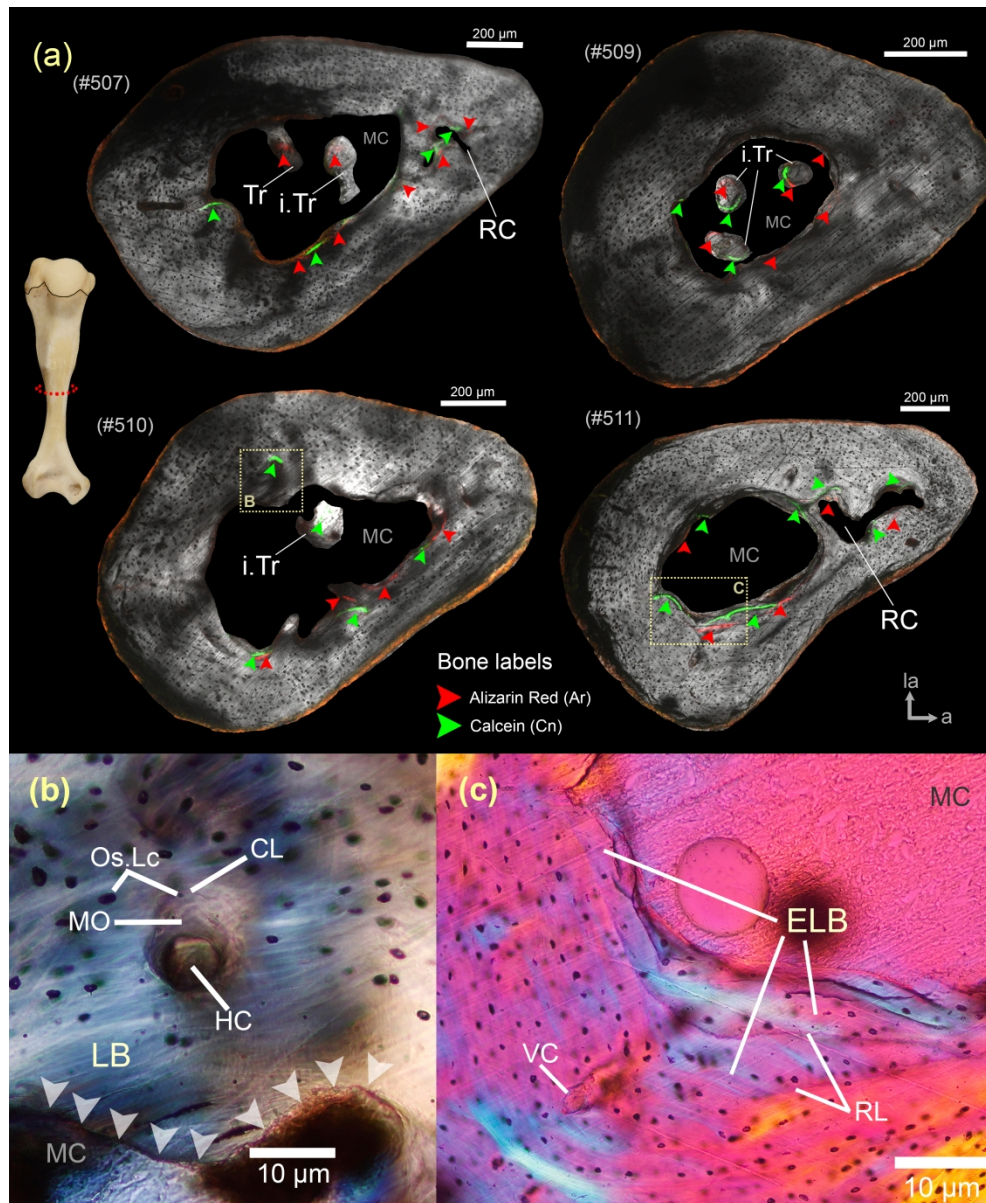
Figure 2. Fluorochrome bone labeling in the humerus of subordinate naked mole-rats. A) Distribution of double labels in endocortical and intracortical regions of four females indicated by red (Ar) and green (Cn) arrow-heads. B) Formation of a secondary osteon (SO) and detail of its Haversian canal (HC). The osteocyte lacunae (Os.Lc) of the SO are smaller than the Os.Lc of the surrounding lamellar bone (LB) matrix. Arrow-heads indicate endosteal resorptive surfaces (lateral side). C) Fluorochrome labels were detected in areas of endosteal lamellar bone (ELB) (medial side). Abbreviations: anterior side (a), cement line (CL), isolated trabeculae (i.Tr), lateral side (la), medullary cavity (MC), mineralized osteoid (MO), resorption cavity (RC), resorption line (RL), trabeculae (Tr), vascular canal (VC).
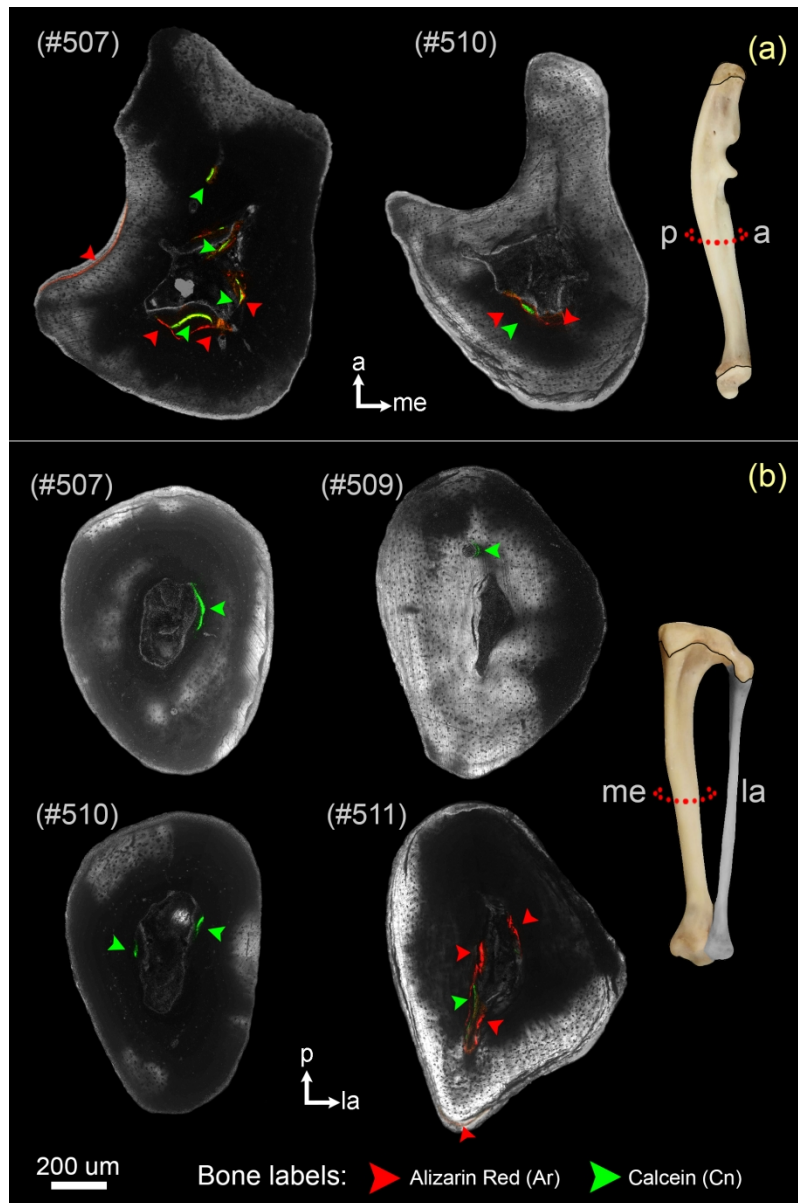
Figure 3. Fluorochrome bone labeling in the ulna (A) and tibia (B) of subordinate naked mole-rats. Bone labels were less evident in these bones and were mostly restricted to endocortical regions. Abbreviations: anterior (a), lateral (la), medial (me), posterior (p).
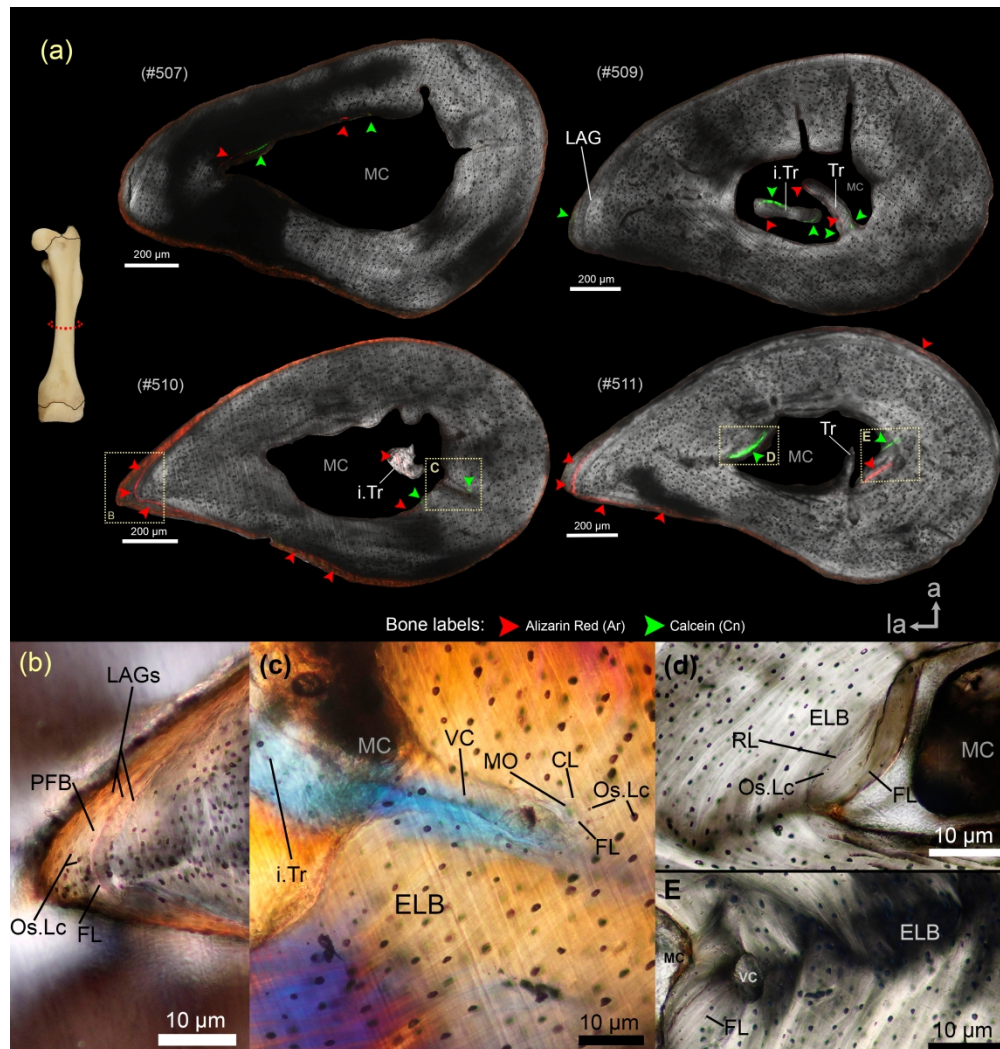
Figure 4. Fluorochrome bone labeling in the femur of subordinate naked mole-rats. A) Four females showing endocortical, intracortical and pericortical distribution of double labels. Periosteal labels were recorded mostly in the tip of the lateral side, where lines of arrested growth (LAGs) were also observed. B) Detail of LAGs in the lateral tip of the femur (#510). A fluorochrome label (FL) of Alizarin red (Ar) was deposited along with this growth mark. C) Remodeling of an eroded vascular canal (VC) (endocortical region). D) Calcein (Cn) labels were deposited in endosteal lamellar bone (ELB) (lateral side). E) Double labels were deposited in ELB (medial side). Abbreviations: anterior side (a), cement line (CL), isolated trabeculae (i.Tr), lateral side (la), medullary cavity (MC), mineralized osteoid (MO), parallel-fibered bone (PFB), osteocyte lacunae (Os.Lc), resorption cavity (RC), trabeculae (Tr).
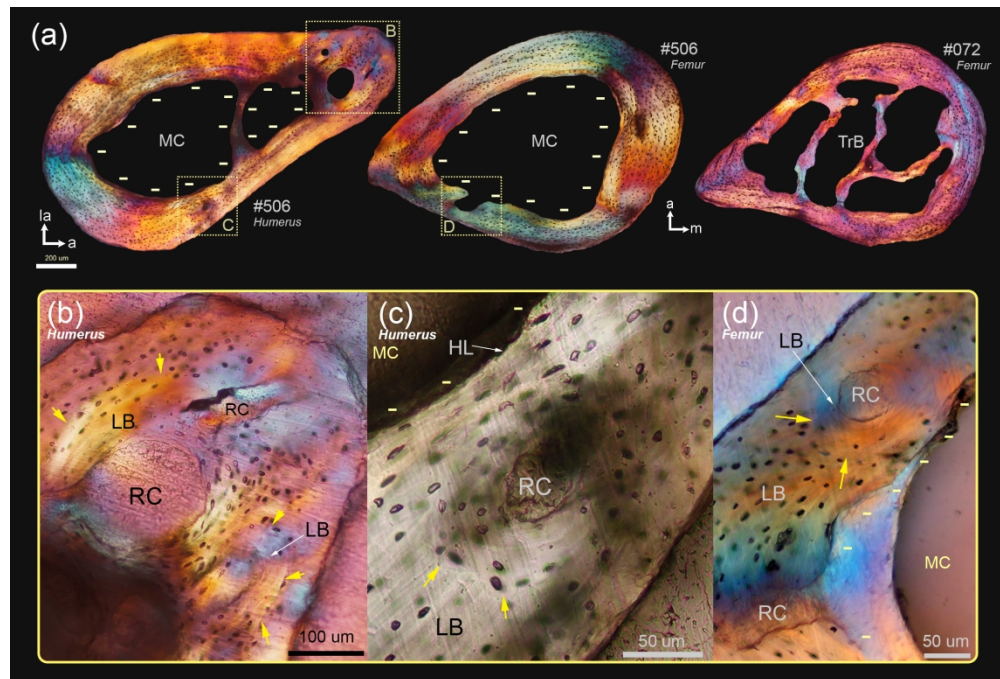
Figure 5. Bone remodeling in female breeders. A) Humeral and femoral cross-sections of reproductive females showing high variation in cortical microanatomy, e.g. relatively thinner cortical walls, increased endosteal bone resorption (-) and larger medullary cavities (MC) as compared to subordinates (compare with Figures 2A, 4A). The femur of the specimen #072 developed highly trabecularized bone (TrB) in the MC. B) Detail of the anterolateral side of the humerus (#506) showing enlarged resorption cavities (RC) with secondary reconstruction. Yellow arrow-heads indicate resorption lines. C) Medial side of the humerus (#506) showing detail of secondary osteons (SO). The cement line is indicated by yellow arrow-heads. Note the different orientation and size of the osteocyte lacunae within the SO with respect to the osteocyte lacunae of the surrounding lamellar bone (LB) matrix. This indicates a change in bone tissue arrangement and therefore secondary centripetal infilling. Both the Haversian canal and the endosteal margin of the bone are under resorption (-), which is evidenced by the presence of Howship's lacunae (HL). D) Detail of a SO formed in the posterior side of the femur (#506). Endosteal resorption (-) is also observed. For a better visualization, this image was vertically inverted.